Physica 8D (1983) 303–342
North-Holland Publishing Company

UNIVERSAL PROPERTIES OF THE TRANSITION FROM QUASI-PERIODICITY TO CHAOS IN DISSIPATIVE SYSTEMS

Stellan OSTLUND*, David RAND†, James SETHNA* and Eric SIGGIA*
Institute for Theoretical Physics, University of California, Santa Barbara, Santa Barbara, CA 93106, USA

Received 30 September 1982
Revised 25 March 1983

An exact renormalization group transformation is developed for dissipative systems which describes how the transition to chaos may occur in a continuous and universal manner if the frequency ratio in the quasi-periodic regime is held at a fixed irrational value. Our approach is a natural extension of K.A.M. theory to strong coupling. Most of our analysis is for analytic circle maps. We have found a strong coupling fixed point where invertibility is lost, which describes the universal features of the transition to chaos. We find numerically that any two such critical maps with the same winding number are C^1 conjugate. It follows that the low frequency peaks in an experimental spectrum are universal and we determine how their envelope scales with frequency.

When the winding number has a periodic continued fraction, our renormalization transform has a fixed point and spectra are self similar in addition. For a set of non-periodic winding numbers with full measure our renormalization transformation yields an ergodic trajectory in a sub-space of all critical maps. Physically one finds singular and universal spectra that do not scale.

Contents

* On leave from Laboratory of Atomic and Solid State Physics, Cornell University, Ithaca, NY 14853, USA.
† On leave from Mathematics Institute, University of Warwick, Coventry CV4 7AL, England.

1. Introduction

In this paper we show how a quasi-periodic flow, with two sharp incommensurate frequencies, can be made to bifurcate to a chaotic or turbulent state in a quantitatively universal way. The transition we envisage is a continuous one and our analyses make essential use of renormalization group methods which were first introduced in the context of dynamical systems by Feigenbaum [1]. There are now many experiments in low aspect ratio systems that observe quasi-periodic behavior prior to the onset of turbulence [2]. Usually, however, the actual transition is preceeded by mode locking in which the ratio of the two basic frequencies, ω_1 and ω_2, sticks at a rational value for some range of parameters. The observed flow is then periodic.

A number of reasonable conjectures can then be made about how the invariant 2-torus in phase space on which the quasi-periodic motion takes place breaks down and gives rise to turbulence. Although the actual events that precede this transition are quite complex (and are left for an appendix), in the absence of period doubling there do not appear to be any quantitative and universal features that could be measured in a real experiment. Thus it is difficult to test these conjectures.

We therefore discuss how to modify the experiments, in a tractable way, so as to make the transition from quasi-periodicity to turbulence occur directly and yield a clear experimental signature. Our proposal requires that two experimental parameters be controlled in a consistent way. (In the jargon, the transition is then said to be of co-dimension two.) Typically one just varies one (i.e., the Rayleigh or Reynolds' number) which explains why this transition has not been seen before.

Since it will emerge that the transition to turbulence approached in this way is universal, it is sufficient to study only the simplest nontrivial dynamical model. Clearly the model must possess an attracting invariant 2-torus to describe quasi-periodicity. Theoretically, it is then convenient to look at successive intersections of this flow with a suitably chosen surface (the Poincaré section) and to work only with maps. Since the universal features of the transition reside only in the long time behavior of the system no essential information is thereby lost. In an experiment in which the second frequency, ω_2, is introduced by means of a periodic external force, the same reduction could be accomplished by observing the quasi-periodic system every $2\pi/\omega_2$ sec. On the map, the invariant torus becomes an invariant circle.

A model system rich enough to include the transition we intend to study is the following family of invertible analytic maps of the annulus:

$$\begin{aligned} P_{\omega,a}(r, \phi) = (&1 + \lambda(r-1) - (a/2\pi)\sin(2\pi\phi)\,, \\ &\phi + \omega + \lambda(r-1) - (a/2\pi)\sin(2\pi\phi))\,, \end{aligned} \tag{1.1}$$

where $0 < \lambda < 1$ and r and ϕ are polar coordinates. It will be useful to note that for infinite contraction ($\lambda = 0$), (1.1) reduces to an analytic map of the circle

$$\phi' = \phi + \omega - (a/2\pi)\sin(2\pi\phi)\,. \tag{1.2}$$

The remaining two parameters are both relevant to our analysis; a controls the nonlinearity and is akin to the Reynolds' number, and ω sets the rotation rate. By the latter we mean just the mean rotation rate of ϕ per iteration which in the quasi-periodic regime is just ω_1/ω_2. (A precise definition is given below.)

When $a = 0$, $r = 1$ is an attracting invariant circle and $P_{\omega,a}$ is a pure rotation with rotation number ω. In fact, this circle is normally hyperbolic [3] and it may therefore be proven that for small values of a this circle persists although the flow on it may be mode-locked. Since $P_{\omega,a}$ contracts areas uniformly, (its Jacobian is λ), any invariant curve is unique. Let $\rho = \rho(\omega, a)$ be the rotation number of the restriction $f_{\omega,a}$ of $P_{\omega,a}$ to this invariant circle. We now ask how this curve breaks down as the nonlinearity is increased.

To refine this question we need to consider the

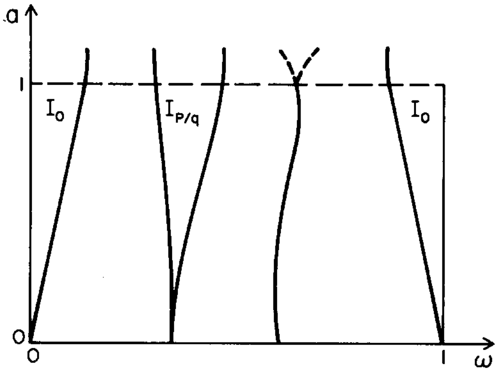

Fig. 1. General structure of the parameter space for the analytic circle homeomorphism (1.2). The regions $I_{p/q}$ are mode-locked with rotation number p/q while the continuous curves represent irrational rotation numbers.

bifurcation structure in the (ω, a) parameter space. For small coupling, $0 < a \ll 1$, the picture follows from the small divisor perturbation theory of Kolmogorov, Arnold and Moser [4, 5, 6] The regions $I_{p/q}$ of parameter space where $\rho(\omega, a) = p/q$ (p, q integers) and where $f_{\omega,a}$ has an orbit of period q are tongues of the general form shown in fig. 1. Each tongue intersects the line $a = \text{const.} > 0$ in a nontrivial closed interval. Between the tongues are curves of the form $\omega = u(a)$, (u a continuous function) on which ρ is irrational and where $f_{\omega,a}$ is conjugate through a continuous change of variables to a trivial rotation. The union of these curves has positive Lebesque measure. The $I_{p/q}$ are the phase locked regions.

One lesson of small divisor theory is that it is sensible to use the parameter ω to control ρ so that we can increase the coupling a and keep ρ fixed at a suitable irrational value.

Under these circumstances there is good evidence (to be presented here and in ref. 11) for the existence of a critical value of $a = a^*$ such that for $a < a^*$ there is an analytic invariant circle, which becomes nonanalytic at $a = a^*$ and ceases to exist for $a > a^*$. The radius of convergence shrinks smoothly to zero as a approaches a^* from below and our renormalization group is designed to extract the universal scaling properties of the critical curve at $a = a^*$. Knowledge of the conjugacy which relates the singular invariant curve to the pure rotation is equivalent to determining the long time behavior of iterates of the map and thus the low frequency peaks in an experimental spectrum. One result of our analysis will be to show that all the frequency peaks are universal and to calculate their relative amplitudes at $a = a^*$.

The analysis necessary to extract the universal data at $a = a^*$ encoded in high iterates of the annular map is enormously simplified by realizing that we can restrict our attention to maps of the circle. The reduction in dimension from an annulus to a circle is ultimately due to the dissipation. Of course the annular map could be expanding in some region provided only that the average contraction rate along the invariant curve is positive. The contraction rate of the nth iterated map then approaches n-times the mean contraction rate. More precisely, there will be uniform exponential convergence onto the invariant curve along directions that intersect it transversely. Thus the annular map is only nontrivial in the direction along the invariant curve. For $a \ll a^*$ one can sensibly define an analytic and invertible circle map as the restriction of the annular map (or some fixed iterate thereof) to the invariant curve.

Unfortunately for our purposes this simple construction is not uniformally appropriate as $a \to a^*$. To understand the difficulty, assume the mechanism for the smooth loss of analyticity at a^* is a tangency between the contracting direction and the invariant curve. Baring accidental symmetries there should be a preferred phase ϕ^* where the angle between the two is minimal as $a \to a^*$. Examination of a high iterate of the map in the limit of zero angle reveals zero slope of ϕ^* in the associated circle map. The difficulty in our construction is that to achieve contraction onto the invariant curve requires an infinite number of iterates which spread the points of zero derivative, generically inflections, densely around the circle. We would like to claim that the circle map so obtained is equivalent to performing the same iterations on an analytic circle map with a single point of zero slope at ϕ^*.

This delicate point as far as we can see can only be established with the aid of the renormalization group developed here. The complication of an infinite number of inflection points is avoided by dilating, expanding and truncating the domain of definition after each iteration so as to retain only the inflection point at ϕ^*. The difficult step is to show that iterates of the annular map under the same process of dilating and truncating are described by the same limiting function as characterizes circle maps. The limiting annular map has the desired property that the foliation is tangent to the invariant curve at only one point in the reduced domain and further that the contraction rate in one iteration is infinite. To make the presentation coherent we develop our formalism for circle maps first and defer applications to annular maps to the very last section.

In the next section we discuss some of what is known mathematically about analytic homeomorphisms of the circle (e.g., (1.2)). We then ask how large iterates of the map scale. When the inverse homeomorphism is differentiable the answer to this question follows simply from deep results of Arnold and Herman [4, 7, 8]. However, when the map in question develops a cubic inflection point (i.e., just at the point where it becomes noninvertible) a different scaling is found. This is reflected in the structure of the nonanalytic invariant circle at the onset of chaos. Section 2 concludes with a synopsis of our numerical results for inflectional maps which were found independently by Shenker [9, 10, 11].

In section 3 we define a renormalization group which reduces questions of scaling and universality to the existence of a fixed point with certain stability properties. In section 4 we solve for this fixed point numerically and discuss the flows induced by our renormalization group transformation. By linearizing around the fixed point we recover the exponents previously found by directly iterating the map.

In section 5, as a prerequisite to examining spectra, we establish a connection between the functional transformation generated by our renormalization group and the more conventional description in terms of a conjugate homeomorphism familiar from K.A.M. theory. A number of precise conjectures concerning the degree of smoothness of homeomorphisms relating maps with an inflection point are formulated. The universal features expected in the Fourier spectrum of an experimental time-series are identified in section 6. The overall scaling properties of such spectra are also demonstrated.

In section 7 we consider situations in which our renormalization transformation has no fixed point yet there are singular and universal spectra. The notion of an ergodic renormalization group trajectory in function space and its Liapunov exponents is discussed. Section 8 indicates how to extend our renormalization group to two-dimensional maps such as (1.1). In the conclusion, we consider how to experimentally test our predictions and mention several other small divisor problems that may be treated by renormalization group methods. Related results have been independently obtained by Feigenbaum, Kadanoff and Shenker [11].

The appendix collects mathematical results for non-invertible maps of the circle and annular maps with particular attention to the qualitative question of how the transition from a mode locked state to chaos occurs when the rotation number is not controlled.

2. Maps of the circle

Firstly, we discuss the well known mathematical theory for diffeomorphisms of the circle. Then we describe the scaling relations obtained in numerical experiments for analytic maps of the circle with a single inflection point which is cubic (we call these *cubic critical maps*). We leave to section 4 the explanation of these relations in terms of a renormalisation transformation and to section 6 and the appendix the justification of the connection with the transition from quasi-periodicity.

2.1. *Generalities and the rotation number*

We shall represent the circle T^1 as the real numbers mod 1 and denote the real line as $\mathbb{R}$. A homeomorphism of T^1 (resp. $\mathbb{R}$) is a continuous mapping of T^1 (resp. $\mathbb{R}$) onto itself with a continuous inverse. An analytic (resp. C^r, $1 \leqslant r \leqslant \infty$) diffeomorphism is an analytic (resp. C^r) homeomorphism with an analytic (resp. C^r) inverse. Every homeomorphism of T^1 can be represented by a homeomorphism f of $\mathbb{R}$ such that $f(\theta+1) = f(\theta) + 1$; the associated circle homeomorphism is then $\theta \to f(\theta) \bmod 1$. We denote the class of such homeomorphisms of $\mathbb{R}$ by $\mathscr{D}_0$.

The rotation number of $f \in \mathscr{D}_0$ is

$$\rho(f) = \lim_{n\to\infty} n^{-1}(f^n(\theta) - \theta)\,. \tag{2.1}$$

This limit exists and is independent of θ. Another useful characterisation is this:

$$\sigma = \rho(f) \Leftrightarrow |f^n(\theta) - \theta - n\sigma| < 1, \quad \text{for all } n, \theta\,. \tag{2.2}$$

(In terms of the original quasi-periodic flow, ρ is the ratio of two fundamental frequencies – consequently it is accessible experimentally.)

Some elementary facts about ρ are these:

a) if $R_\lambda(\theta) = \theta + \lambda$, then $\rho(R_\lambda) = \lambda$;

b) if $f \in \mathscr{D}_0$ and $\rho(f) = p/q$ then there exists θ such that $f^q(\theta) = p + \theta$ and θ mod 1 is a periodic point of the associated circle homeomorphism;

c) ρ depends continuously on $f \in \mathscr{D}_0$ in the C^0-topology: this means that, given f, if $\epsilon > 0$ there exists $\delta > 0$ such that $\sup_\theta |f(\theta) - g(\theta)| < \delta$ implies $|\rho(f) - \rho(g)| < \epsilon$.

d) if f_μ is the 1-parameter family given by $f_\mu = R_\mu \circ f$ then $\rho(f_\mu)$ is an increasing function of μ and is strictly increasing at points where ρ is irrational [7].

2.2. *Conjugation to a rotation*

Consider the map $\theta \to f(\theta)$ where $f \in \mathscr{D}_0$. On making the coordinate change $\theta = h(\phi)$, $h \in \mathscr{D}_0$, this map becomes $\phi \to h^{-1}fh(\phi)$. We say that f and g are conjugate (resp. analytically conjugate) if there exists a homeomorphism (resp. analytic diffeomorphism) h such that $g = h^{-1}fh$. It immediately follows from (2.2) that two conjugate homeomorphisms have the same rotation number. A basic problem is to determine when the converse holds and, in particular, to determine when $f \in \mathscr{D}_0$ is conjugate (or better analytically conjugate) to $R_{\rho(f)}$. Then every orbit of R_σ is dense in T^1. And f is conjugate to R_σ if f has an orbit $\{f^n(\theta)\}_{n=0}^\infty$ which is dense in T^1 because then we can define h by the condition that $h(n\sigma) = f^n(\theta)$. Denjoy [12] has shown that if $\log(f')$ is of bounded variation and $\sigma = \rho(f)$ is irrational then every orbit of f in T^1 is dense. This condition is satisfied by C^2 diffeomorphisms with irrational rotation number.

Note that the above argument shows that if h exists then it is unique up to a translation. Thus for a given f one can ask how smooth h is. The following basic result about this is due to Herman [7]: there exists a set [13] $A \subset [0, 1]$ with Lebesgue measure one such that, if f is an analytic diffeomorphism and $\sigma = \rho(f) \in A$, then f is analytically conjugate to R_σ. For our purposes it is sufficient to note that A contains those numbers with bounded entries in their continued fractions.

2.3. *Continued fractions and scaling*

We now consider analytic diffeomorphisms f with irrational rotation number $\sigma = \rho(f)$. Since we are interested in the rational approximations of σ it is convenient to express it as a continued fraction:

$$\sigma = \cfrac{1}{n_1 + \cfrac{1}{n_2 + \ddots}} = [n_1, n_2, n_3, \ldots]\,. \tag{2.3}$$

Within the set of all rational numbers whose denominator does not exceed a given bound, the best rational approximation to σ is

$$p_m/q_m = [n_1, n_2, \ldots, n_m, n_{m+1} = \infty] .$$

We use this notation henceforth. For the rest of this section we restrict ourselves to the case where $n_{m+s} = n_m$ for some $s \geqslant 1$. This condition is imposed so that we can speak of self similarity for appropriate iterates of the map.

Define $\tau = \lim_{n\to\infty} q_{n+s}/q_n$. When $s = 1$, $\tau = \sigma^{-1}$.

By Herman's Theorem [7] we have that f is analytically conjugate to R_σ where $\sigma = \rho(f)$, i.e. $f^{q_n} = hR_{q_n\sigma}h^{-1}$ with h an analytic diffeomorphism. Consequently, $f^{q_n} - p_n = h(R_{q_n\sigma} - p_n)h^{-1}$ converges to the identity as $n\to\infty$. Moreover, for large n, $f^{q_n}(0) - p_n$ is closer to 0 than $f^k(0) - l$ for all $1 \leqslant k < q_n$ and $l = 0, 1, 2, \ldots$. Because the points $f^{q_n}(0) - p_n$ and $R_{q_n\sigma}(0) - p_n$ are related by this analytic coordinate change;

$$\alpha^s = \lim_{n\to\infty} (f^{q_n}(0) - p_n)/(f^{q_{n+s}}(0) - p_{n+s})$$
$$= \lim_{n\to\infty} (R_{q_n\sigma}(0) - p_n)/(R_{q_{n+s}\sigma}(0) - p_{n+s}) = (-)^s\tau . \tag{2.4}$$

Let $1/\alpha^{(n)} = (f^{q_n}(0) - p_n)/\sigma$ and let $\lambda_a(\theta) = a\theta$. Note that $\lim_{n\to\infty}(\alpha^n/\alpha^{(n)})$ exists and is nonzero.

Lemma 2.1. As $n\to\infty$, $\lambda_{\alpha(n)}(f^{q_{ns}} - p_{ns})\lambda^{-1}_{\alpha(n)}$ converges as an analytic function to R_σ on any bounded domain.

Proof. Let B_δ denote $\{z\in\mathbb{C}: |\mathrm{Im}\, z| < \delta\}$. Since f and h are analytic there exists $\delta > 0$ and analytic extensions $\bar{f}$ and $\bar{h}$ of f and h to B_δ so that for $z\in B_\delta$, $\bar{f}\circ\bar{h}(z) = \bar{h}(z+\sigma)$. We have to prove that

$$\lim_{n\to\infty} \sup_{\substack{z\in B_\delta \\ -A<\mathrm{Re}\, z<A}} |\alpha^{(n)}(\bar{f}^{q_n}(z/\alpha^{(n)}) - p_n) - R_\sigma(z)| = 0 , \tag{2.5}$$

where A serves to delimit an arbitrary finite interval independent of n.

Let $z/\alpha^{(n)} = \bar{h}(y)$ and observe that

$$\bar{f}^{q_n}(\bar{h}(y)) - p_n = \bar{h}(y) + \bar{h}'(y)(q_n\sigma - p_n) + \mathcal{O}(\alpha^{-2n}) .$$

Elimination of y in favor of z together with the observation that $\sup(y)\to 0$ as $n\to\infty$ implies

$$\alpha^{(n)}(\bar{f}^{q_n}(z/\alpha^{(n)}) - p_n) - R_\sigma(z)$$
$$= \alpha^{(n)}(q_n\sigma - p_n)h'(0) - \sigma + \mathcal{O}(\alpha^{-n}) .$$

The definition of $\alpha^{(n)}$ then insures that the right-hand side is $\mathcal{O}(\alpha^{-n})$.

Q.E.D.

It is worth noting that to obtain a universal limit for f^{q_n} and in particular R_σ the scale factor itself had to depend on f, i.e., we used $\alpha^{(n)}$ and not α^n. When we consider cubic critical maps we again will have to make a non-universal scale change to obtain a universal limiting function which replaces R_σ in (2.5). The analogue of $\lim_{n\to\infty} \alpha^{(n+s)}/\alpha^{(n)} = \alpha^s$ will again exist and be universal.

A second scale δ can be defined by asking how quickly diffeomorphisms with a p_n/q_n-cycle approach f. More precisely, let $f_\lambda = R_\lambda\circ f$ and let $\lambda_n(f)$ be the value of λ closest to 0 such that $\rho(f_\lambda) = p_n/q_n$. Then if f is an analytic diffeomorphism (with $\rho(f) = \sigma$ of course), it follows from Herman's results [7] that

$$\delta = \lim_{n\to\infty} \lambda_n(f)/\lambda_{n+s}(f) = -\tau^2 .$$

In the special case where the family is given by (1.2),

$$\delta = \lim_{n\to\infty} (\omega_{n+s} - \omega_n)/(\omega_n - \omega_{n-s}) , \tag{2.6}$$

where for a given value of a ($|a| < 1$), it is convenient to define ω_n as the value of ω such that 0 is contained in a q_n-cycle with rotation number p_n/q_n. (The same definition of δ is used for $|a| = 1$.) Thus δ measures how quickly the phase-locked tongues $I_{p/q}$ converge onto the curve $\rho(f_{\omega,a}) = \sigma$ in $0 \leqslant \omega < 1$, $|a| \leqslant 1$. A third rescaling factor γ will be needed in sections 4–5 to describe how maps that are nearly critical renormalize toward the weak coupling fixed point.

The notation δ was chosen in partial analogy to Feigenbaum's study [1] of period doubling where a single exponent described both the accumulation of periodic 2^n cycles and the onset of chaos. Our problem is codimension two (i.e., there are two relevant directions) which requires us to define both δ and γ.

2.4. *Scaling for cubic critical maps*

We now consider the scaling relations for cubic critical maps analogous to (2.4) and (2.5). These were discovered by us, and independently, by Shenker, in computer experiments mainly on the family (1.2) [9, 10]

$$\theta \to f_\omega(\theta) = \theta + \omega - (a/2\pi)\sin(2\pi\theta)\,. \qquad (2.7)$$

Our conventions are arranged such that (2.7) has a cubic critical point at 0 for $a = 1$. We will look for scaling around the origin since it is known from general theorems (appendix) that knowledge of the orbit of the critical point largely determines the dynamics of the map. The numerical method used is similar to that of Greene [14]. We worked mainly with the irrational winding number that is most poorly approximated by rationals, $\sigma = \sigma_G = (\sqrt{5}-1)/2$ for which $n_i = 1$ and $q_1 = 1$, $q_2 = 2$; $q_{n+1} = q_n + q_{n-1}$ and $p_n = q_{n-1}$.

By solving the equation $f^{q_n}_{\omega_n}(0) = p_n$ for ω_n we can estimate δ from its definition (2.6). With 14-figure arithmetic and $\sigma = \sigma_G$, ω_n reached its limiting value for $n = 28$ ($q_{28} = 514229$). The corresponding value of α was estimated from the analogue to (2.4), i.e.

$$\alpha = \lim_{n\to\infty} (f^{q_{n-1}}_{\omega_\infty}(0) - p_{n-1})/(f^{q_n}_{\omega_\infty}(0) - p_n)\,. \qquad (2.8)$$

In the same calculation we also determined the function

$$\zeta(x) = \lim_{n\to\infty} \alpha^{(n)}(f^{q_n}_{\omega_\infty}(x/\alpha^{(n)}) - p_n)\,, \qquad (2.9)$$

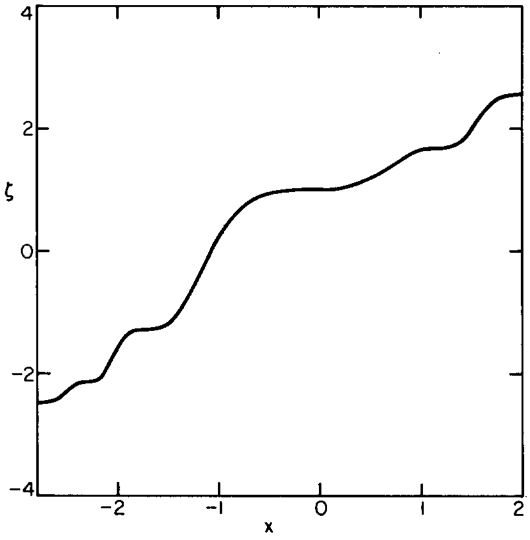

Fig. 2. The universal scaling function (2.9) for $\rho(f) = \sigma_G$ computed from (2.7) at $a = 1$.

where the scale factor $\alpha^{(n)}$ was determined by insisting that $\zeta(0) = 1$ for each approximate n.

The finite n approximations to α and ζ continued to improve out to $n = 17$ ($q_{17} = 2584$). From the fluctuations between successive cycles we estimate the error in ζ (fig. 2) to be 2×10^{-5} using the L1 norm over the interval bounded by the two inflection points that bracket the origin. We also found $\alpha = -1.28862 \pm 0.00005$ and $\delta = -2.83361 \pm 0.00001$. We believe our limiting error reflects just the loss of accuracy due to the cubic inflection point together with a machine accuracy of 10^{-14}. Table I contains a synopsis of our numerical results for other winding numbers and maps. From this one sees that ζ as well as the scale factors α and δ depend on the rotation number and the order of the critical inflection point (e.g., cubic) but are otherwise universal and independent of other details of the map.

2.5. *Fixed point equations* ($\sigma = \sigma_G$)

From the definition of ζ in (2.9) and the relations $f^{q_{n+1}} = f^{q_n} \circ f^{q_{n-1}} = f^{q_{n-1}} \circ f^{q_n}$ one sees that ζ must

TABLE I

The scaling factors α and δ for the critical sine map (2.7) and the power map (2.11) with a cubic inflection point and for the winding numbers indicated. Note that the scale factor corresponding to a full period of the continued fraction is α^s by (2.4). The convergence to a universal value with the order of the rational approximate is clearly oscillatory for both α and δ. No attempt to model the error term was made although it might have added one significant digit to our values. The quoted error is large enough to bracket three successive values of the parameter. We also verified, although with lesser accuracy, that for $\rho = \sigma_G$ when $b \to 1$ in (2.11) $-\alpha$ tends smoothly to $1/\sigma_G$. Specifically for $b = 2$, 1.3, 1.1, and 1.02, $-\alpha = 1.388 \pm 0.002$, 1.474 ± 0.002, 1.5817 ± 0.0002, 1.6103 ± 0.0002. The corresponding $-\delta$ values are 2.7078, 2.6494, 2.61978, 2.618108 ± 0.000003 and 2.618052 ± 0.000002 for $b = 1.01$. In the opposite limit of $b \to \infty$, $-\alpha \to 1$, e.g., for $b = 4$, 8, 16, $-\alpha = 1.231 \pm 0.002$, 1.131 ± 0.005 and 1.071 ± 0.002.

Equation (2.7)			
ρ	$1, 1, 1, \ldots$	$2, 2, 2, \ldots$	$1, 2, 1, 2, \ldots$
$-\alpha$	1.28862 ± 0.00005	1.5868 ± 0.0001	1.4032 ± 0.0002
$-\delta$	2.83361 ± 0.00001	6.79925 ± 0.00005	17.66906 ± 0.00002
Equation (2.11)			
ρ	$1, 1, 1, \ldots$	$2, 2, 2, \ldots$	$1, 2, 1, 2, \ldots$
$-\alpha$	1.2885 ± 0.0003	1.5865 ± 0.0005	1.4033 ± 0.0002
$-\delta$	2.833 ± 0.002	6.795 ± 0.005	17.670 ± 0.005

satisfy the equations

$$\zeta(\theta) = \alpha\zeta(\alpha\zeta(\theta/\alpha^2)) \tag{2.10a}$$

and

$$\zeta(\theta) = \alpha^2\zeta(\alpha^{-1}\zeta(\theta/\alpha)). \tag{2.10b}$$

Feigenbaum et al. [11] have numerically solved (2.10) and found nontrivial solutions. However, (2.10) is rather confusing because, as we shall see from our renormalisation group analysis, (2.10b) is essentially redundant and (2.10a) alone specifies ζ up to a scale change [15]. Also, this approach becomes very cumbersome when one deals with other winding numbers as the equations corresponding to (2.10) become more numerous and more complicated. The renormalisation transformation constructed in the next section provides a clear computational tool for calculating ζ as well as an explanation of its existence (cf. (3.6)).

2.6. *Other critical maps*

We have also investigated a number of non-analytic functions of the form

$$\theta \to f(\theta) = \omega + \theta|2\theta|^{b-1}, \tag{2.11}$$

where $\theta \in [-\frac{1}{2}, \frac{1}{2}]$. In each case we obtain good convergence for α, δ and ζ but now these depend on the value of b. The entries in table I for $b = 3$ are a check that α and δ are universal for generic critical maps even when the map in question is not an analytic homeomorphism (e.g., (2.11)).

Jonker and Rand [16] have proven by means of the renormalization group transformation in the following section that α and δ are analytic functions of $b - 1 = \epsilon$ for small ϵ. This makes unambiguous the numerical determination of the leading coefficient in an ϵ-expansion. Specifically for $\rho = \sigma_G$, $-\alpha = 1/\sigma_G - 0.37\epsilon$ and $-\delta = \sigma_G^{-2} + 0.19\epsilon^2$ with errors of order 5% in the coefficients.

3. Renormalization group analysis of circle homeomorphisms

We now give an explanation of the above phenomena by implementing a renormalisation group analysis along the general lines developed by Feigenbaum in his study of period doubling [1, 17]. Our construction is slightly more complicated than Feigenbaum's since it depends upon rotation number and our orbits are not periodic. Nevertheless, our transformation is defined on an open set of maps that does not constrain the winding number.

The great utility of the renormalisation group in dynamical systems has been to reduce questions of existence and universality to a geometric problem in function space, which, for period doubling, has been brought under sufficiently quantitative control to permit mathematical proofs [17, 18, 19]. An additional virtue of the renormalisation group for our problem is that the universal features of the spectra will follow from the coordinate change that reduces our fixed point homeomorphism f_* to a rotation. There is no need to work backwards from f_*, which controls the iterates near the inflection point, to recover the rest of the orbit.

Although our main interest is with the class of *cubic critical mappings* of the circle (i.e., analytic maps with a unique inflection point which is cubic), it turns out that to construct a renormalisation transformation we have to work in a larger space of suitably constrained pairs of analytic homeomorphisms of the line. After studying the renormalisation transformation in this bigger space, we obtain the scaling properties etc. of the analytic mappings by considering how they are embedded in this space and how the transformation acts upon them.

Each element of this bigger space naturally defines a piecewise analytic map of the circle. This is extremely useful because it allows an immediate definition of rotation number and more importantly enables us to construct conjugating homeomorphisms which play an important role in our demonstration of the universality of the spectrum. These conjugacies possess unexpected properties which are shared by both analytic and our piecewise analytic circle mappings.

The renormalisation group transformation T_n applied to a particular circle homeomorphism f (and the space we embed it in) depends upon $n = n_1$ where

$$\rho(f) = \cfrac{1}{n_1 + \cfrac{1}{n_2 + \cdots}} = [n_1, n_2, \ldots], \tag{3.1}$$

i.e., n_1 is such that $n_1 \leqslant 1/\rho(f) < n_1 + 1$. In this way arbitrary rotation numbers can be studied because the image of f under T_n will have rotation number $1/(n_2 + 1/(n_3 + \cdots))$. When the continued fraction (3.1) is periodic, say $n_{i+s} = n_i$, we seek a fixed point of

$$T = T_{n_{s-1}} \circ \cdots \circ T_{n_1} \tag{3.2}$$

and study the structure of T near the fixed point (its linearisation, stable and unstable manifolds, etc.). Associated with this fixed point is the universal 2-parameter family of circle maps which correspond to its unstable manifold.

3.1. *Definitions and formal properties* [20]

We now define T_n and the space $\mathscr{S}_n$ upon which it acts. Let $\mathscr{S}_n$ consist of the pairs (ξ, η) of analytic homeomorphisms of $\mathbb{R}$ which satisfy the following conditions ($' =$ derivative):

$$\begin{aligned}
&\text{(a)} \quad \xi(0) = \eta(0) + 1\,,\\
&\text{(b)} \quad \eta(\xi(0)) = \xi(\eta(0))\,,\\
&\text{(c)} \quad 0 < \xi(0) < 1\,,\\
&\text{(d)} \quad \xi^n(\eta(0)) > 0\,,\\
&\text{(e)} \quad \xi^{n-1}(\eta(0)) < 0\,,
\end{aligned} \tag{3.3}$$

(f) if $\xi'(x) = 0$ or $\eta'(x) = 0$ for x in $[\eta(0), \xi(0)]$ then $x = 0$ and $\eta'(0) = \xi'(0) = \eta''(0) = \xi''(0) = 0$, but $\xi'''(0)$ and $\eta'''(0)$ are nonzero;

and

(g) $(\xi\eta)'(0) = (\eta\xi)'(0)$, and if $\xi'(0) = 0$ then $(\xi\eta)'''(0) = (\eta\xi)'''(0)$.

Let $\mathscr{S}_{n,\text{crit}}$ denote the subset of those (ξ, η) in $\mathscr{S}_n$ with $\xi'(0) = \eta'(0) = 0$. If $\sigma = [n, n_2, \ldots]$ let $S_{\sigma,\text{crit}}$ denote those (ξ, η) in $\mathscr{S}_{n,\text{crit}}$ with $\rho(\xi, \eta) = \sigma$. Note that (a), (b) and (c) imply $\eta(0) < \xi(\eta(0)) < \xi(0)$ and condition (e) is redundant when $n = 1$.

Conditions (a)–(c) permit us to associate a homeomorphism $f = f_{\xi,\eta}$ on the unit circle with each pair $(\xi, \eta) \in \mathscr{S}_n$. Define $f = \xi$ on $[\eta(0), 0]$ and $f = \eta$ on $[0, \xi(0)]$ and associate the unit interval $[\eta(0), \xi(0)]$ with the circle by identifying end points. Fig. 3 illustrates our construction. A rotation number $\rho(\xi, \eta) = \rho(f)$ can be defined for f in the usual way. Conditions (d)–(e) ensure that $n < 1/\rho(f) < n + 1$. Let $\tilde{\mathscr{S}}_n$ be the space of homeomorphisms obtained from $\mathscr{S}_n$ in this manner.

Now define a mapping T_n on $\mathscr{S}_n$ by

$$T_n(\xi, \eta) = (\alpha\xi^{n-1}\eta\alpha^{-1}, \alpha\xi^{n-1}\eta\xi\alpha^{-1}). \tag{3.4}$$

The scale factor $\alpha = 1/(\xi^{n-1}\eta(0) - \xi^n\eta(0))$ obeys $\alpha < -1$ by (d)–(e). Note that the compositions involved are all well defined. This is not the case if ξ and η are interchanged in the right-hand side of (3.4). It is easy to verify that conditions (a)–(c) and (f)–(g) are preserved by T_n. Condition (f) restricts us to cubic critical points and condition (g) eliminates an uninteresting marginal direction at the fixed point (see section 4) and is satisfied by all those (ξ, η) which came from analytic circle mappings since they commute.

The analytic diffeomorphisms and cubic critical maps f are embedded in our space $\mathscr{S}$ as follows: with f we associate the pair $(\xi, \eta) = (f, f - 1)$.

Let $\tilde{T}_n$ be the mapping induced by T_n on $\tilde{\mathscr{S}}_n$. The action of $\tilde{T}_n$ is most conveniently illustrated for the case $n = 1$ (fig. 4). If $f = f_{\xi,\eta} \in \tilde{\mathscr{S}} = \tilde{\mathscr{S}}_1$, then let $f(0^+) = \eta(0)$ and $f(0^-) = \xi(0)$ and define

$$g = \begin{cases} f^2, & \text{on } [f(0^+), 0], \\ f, & \text{on } [0, f^2(0^-)]. \end{cases}$$

Then $\tilde{T}_1 f = \alpha g \alpha^{-1}$ where $\alpha = 1/(f(0^+) - f^2(0^-))$. Returning to the case of arbitrary n it may be

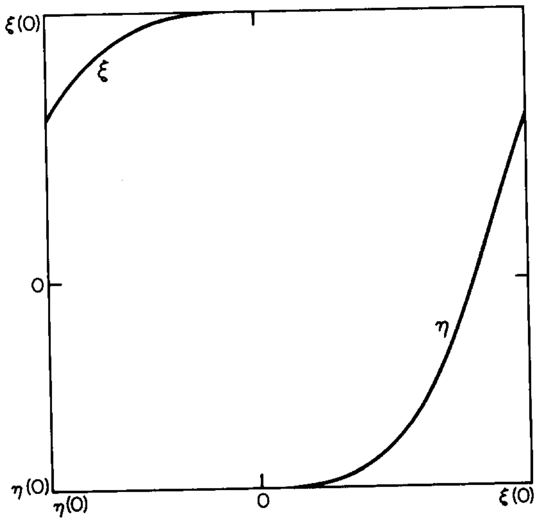

Fig. 3. Construction of a circle homeomorphism from a pair of analytic functions (ξ, η) satisfying conditions (3.3). The functions actually graphed correspond to the fixed point of T_1 and satisfy $\rho(f_{\xi,\eta}) = \sigma_G$.

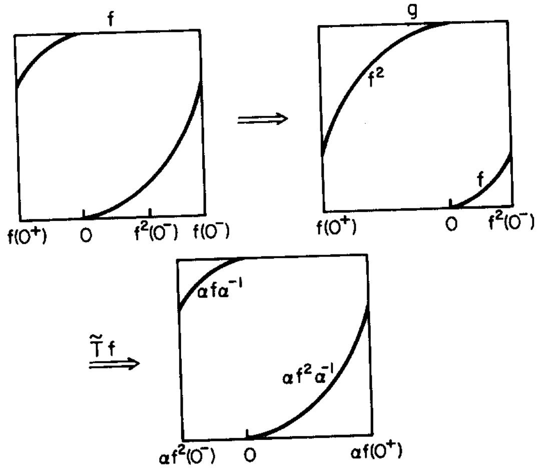

Fig. 4. Illustration of the action of T_1 on f. On the first line f on $[f^2(0^-), f(0^-))$ is iterated to give g defined on a subinterval of $[0, 1)$. A rescaling by $\alpha < -1$ restores this interval to unit length.

shown that if $f = f_{\xi,\eta}$ then $\tilde{T}_n^k(f)$ is given by

$$(\beta^k f^{q_k} \beta^{-k}, \beta^k (f^{q_k + q_{k-1}}) \beta^{-k}),$$

where β is the geometric mean of the first k scalings α.

3.2. *Behaviour of the rotation number under T*

From this construction it may also be shown that $\rho(\tilde{T}_1 f) = (1/\rho(f)) - 1$. Divide the domain of f into three regions $I_1 = [f(0^+), 0)$, $I_2 = [0, f^2(0^-))$, and $I_3 = [f^2(0^-), f(0^-))$ then $f(I_1) = I_3$ and $f(I_3) \subset I_1 \cup I_2$. Consider the orbit under f of any point x that avoids 0. The fraction of points on this orbit that fall in I_1, and thus in I_3, is precisely $1 - \rho(f)$. But from an orbit of f we can construct one for g by eliminating all points in I_3. Thus the map $\tilde{T}_1(f)$ has a fraction of $(1 - \rho(f))/\rho(f)$ positive elements on its orbit.

Q.E.D.

The same argument effectively applies to arbitrary T_n acting on $\mathscr{S}_n$.

Lemma 3.1. If $\rho(\xi, \eta) = 1/(n + 1/(n_2 + \cdots))$ then $\rho(T_n(\xi, \eta)) = (1/\rho(\xi, \eta)) - n$.

Proof. Let $I_0 = [0, \xi(0)]$, $I_l = [\xi^{l-1}\eta(0), \xi^l\eta(0)]$, $l = 1, \ldots, n$, $J_1 = [\xi^{n-1}\eta(0), 0]$ and $J_2 = [0, \xi^n\eta(0)]$. Choose x in J_2 such that $f^k(x) \neq 0$ for all $k \geqslant 0$ ($f = f_{\xi,\eta}$) and let $m(k)$ denote the number of elements of $x, f(x), \ldots, f^{k-1}(x)$ which fall into I_0. Then $\rho(f) = \lim_{k\to\infty} m(k)/k$.

Now choose a sequence k_i such that $k_i < k_{i+1}$ and $f^{k_i}(x) \in J_1$. Let $y = \alpha x$, $1/\alpha = \xi^{n-1}\eta(0) - \xi^n\eta(0)$. Then there are precisely $m(k_i)$ elements of the sequence $x, f(x), \ldots, f^{k_i - 1}(x)$ in I_0 and hence the same number in I_l, $l = 1, \ldots, n$. Thus there are $k_i = nm(k_i)$ in J_1. Consequently, $k_i = nm(k_i)$ points of the sequence $y, (\tilde{T}f)y, \ldots, (\tilde{T}f)^{m(k_i)-1}(y)$ fall in $I_0(\tilde{T}f)$ which proves that

$$\rho(\tilde{T}f) = \lim_{k_i\to\infty} (k_i - nm(k_i))/m(k_i)$$
$$= \frac{1}{\rho(f)} - n\,. \qquad \text{Q.E.D.}$$

We note the following three immediate corollaries of the Lemma for the case $n = 1$ and $\sigma = \sigma_G = [1, 1, \ldots]$ although there are obvious analogues for other periodic continued fractions:

$$\begin{aligned} &\text{(a)} \quad \rho(f) = q_{i-1}/q_i \text{ implies } \rho(\tilde{T}f) = q_{i-2}/q_{i-1}; \\ &\text{(b)} \quad \rho(f) = \sigma_G \text{ if and only if } \rho(\tilde{T}f) = \sigma_G; \\ &\text{(c)} \quad \text{if } T_1^k(\xi, \eta) \in \mathscr{S}_1 \text{ for all } k \geqslant 0, \\ &\qquad \text{then } \rho(f_{\xi,\eta}) = \sigma_G\,. \end{aligned} \tag{3.5}$$

The last statement follows from the transformation properties of ρ and the observation that $(\xi, \eta) \in \mathscr{S}_1$ implies $1 < \rho^{-1}(\xi, \eta) < 2$.

From the above lemma, it only makes sense to search for a fixed point of our renormalisation group transformation when the continued fraction of $\rho(f)$ is eventually periodic. Any integers that precede the periodic part may be removed by application of appropriate T_n. Only the tail of the continued fraction is relevant in determining which nontrivial fixed point might exist. A number of remarks about the application of T_n to maps with nonperiodic winding numbers are reserved for section 7.

3.3. *Fixed points of T*

If $(n_1, n_2, \ldots, n_s)$ are the integers in one period of the continued fraction of $\sigma = \rho(f)$, then one should look for a fixed point in $\mathscr{S}_{n_1}$ of the renormalisation transformation T defined by (3.2). Actually T must possess a *weak-coupling fixed point* corresponding to rotation by σ and we believe a second nontrivial fixed point on $\mathscr{S}_{\sigma,\mathrm{crit}}$ (which we call the *strong-coupling fixed point*) corresponding to the onset of chaos at the breakdown of an invariant torus with rotation number σ. The strong-coupling fixed point and associated eigenvalues are found numerically in the following section for two cases $n_i \equiv 1$ and $n_i \equiv 2$.

Our picture is as follows (fig. 5): The strong-coupling fixed point (ξ_*, η_*) $(\rho(\xi_*, \eta_*) = \sigma)$, has a two-dimensional unstable manifold (corresponding to two eigenvalues δ and γ of the linearization of T at (ξ_*, η_*)) which contains the curve

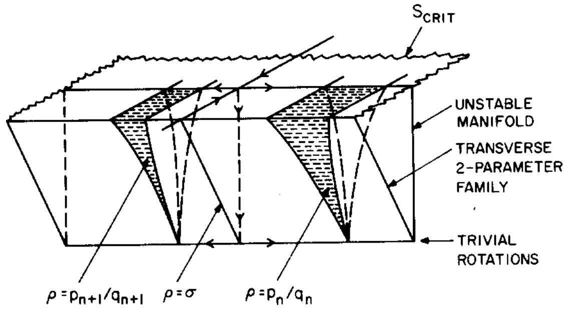

Fig. 5. Schematic representation of the global structure of the dynamics of T in $\mathscr{S}$ showing (a) both fixed points, (b) the universal family corresponding to the unstable manifold of the cubic fixed point, (c) a 2-parameter family of analytic mappings of the circle which is transverse to the stable manifold of the cubic fixed point (e.g., $\theta + \omega - (a/2\pi)\sin 2\pi\theta$), and (d) the relationship between the regions $\rho = \text{const.}$ for the universal and transversal families.

$\{R_\lambda, 0 < \lambda < 1\}$ in its closure. The eigenvalue δ may be found by remaining on $\mathscr{S}_{\text{crit}}$ and asking how maps with $\rho(\xi, \eta) \neq \sigma$ move away from the fixed point as T is iterated. Thus, using (3.5a), it tells how those f with $\rho(f) = \sigma$ are approximated by f with $\rho(f) = p_n/q_n$. To determine γ we can fix $\rho(\xi, \eta) = \sigma$ and examine the flow away from $\mathscr{S}_{\text{crit}}$. The unstable manifold of (ξ_*, η_*) defines a universal 2-parameter family of circle maps.

The stable manifold of (ξ_*, η_*) is of codimension two and consists of all elements of $\mathscr{S}_{\text{crit}}$ with rotation number σ. The structure of a 2-parameter family of analytic maps (such as $f_{\omega,a}(\phi) = \phi + \omega - (a/2\pi)\sin(2\pi\phi)$) which intersects the stable manifold transversely can be related to the universal family by applying T a sufficient number of times. The unstable manifold of the weak-coupling fixed point is the curve $\{R_\lambda, 0 < \lambda < 1\}$ and the stable manifold consists of all non-critical mappings (i.e., diffeomorphisms) with rotation number σ.

Clearly, it is easy to write down the fixed point equation $T(\xi, \eta) = (\xi, \eta)$. When $\sigma = \sigma_G$ so that $T = T_1$ it is

$$\xi = \alpha\eta\alpha^{-1},$$
$$\eta = \alpha\eta\alpha\eta\alpha^{-2}, \tag{3.6}$$
$$\alpha = \frac{\eta(0) + 1}{\eta(0)}.$$

Notice that this is a single equation in a single unknown η.

Lemma 3.2. Let (ξ_*, η_*) be a fixed point of T in $\mathscr{S}_{\text{crit}}$. Then ξ_* and η_* are analytic functions of x^3.

Proof. We show that if $\eta = \eta_*$ the pth derivative $\eta^{(p)}(0) \neq 0$ implies that p is a multiple of 3. A similar result holds if $\xi = \xi_*$. Let $g(x) \equiv \eta(\alpha x)$. Then by (3.6),

$$g(x) = \alpha g\left(g\left(\frac{x}{\alpha^2}\right)\right). \tag{3.7}$$

Differentiating (3.7) three times and putting $x = 0$ one obtains

$$g'(g(0)) = \alpha^5. \tag{3.8}$$

Now assume that the derivative $g^{(p)}(0) = 0$ whenever $p \leqslant 3n$ and p is not a multiple of 3. Let q be such that $3n < q < 3(n+1)$. Differentiating (3.7) q times and setting $x = 0$ one obtains

$$\alpha^{2q-1} g^{(q)}(0) = g'(g(0)) g^{(q)}(0). \tag{3.9}$$

Therefore by (3.8) and (3.9), $g^{(q)}(0) = 0$. Q.E.D.

A similar result holds for the other σ with periodic continued fractions.

Since the stable manifold of (ξ_*, η_*) contains an analytic cubic critical map, the functions ξ_* and η_* commute. A direct proof of this commutation using (3.6) and lemma 3.2 has been given [15] for the case $\sigma = \sigma_G$. Using $\xi_*\eta_* = \eta_*\xi_*$ one directly obtains (2.10b).

3.4. *Existence of a conjugacy to a rotation*

The existence of a strong coupling fixed point and the associated stable manifold has important implications for the orbits of cubic critical maps with the prescribed rotation number. We state our Theorem only for $\sigma = \sigma_G$ though the construction obviously generalizes to other winding numbers along the lines of lemma 3.1. The extension to general periodic σ requires a lower bound on the slope of the fixed point over an interval, which we have only in a compelling way for $\sigma = \sigma_G$.

Theorem 3.1. Let f be in the stable manifold of $f_* = (\xi_*, \eta_*)$ with $\rho(f) = \sigma_G = \sigma$ then it is conjugate to a rotation.

Proof. If f is not conjugate to the rotation R_σ there is a nontrivial closed interval I such that $f^n I \cap I = 0$ for all $n \geqslant 0$ [7]. We call such intervals Denjoy intervals. Assume that f possesses such an interval and let $I(f)$ denote the length of a longest such interval. Note that since f is in the stable manifold, the origin cannot be in a Denjoy interval because as $n \to \infty$, $f^{q_n}(0)$ approaches 0 from both sides. Consequently, $f(0)$ and $f^2(0)$ are not in a Denjoy interval. Let I be a Denjoy interval of maximal length. Then I must be contained in one of the three open intervals on the circle with end-points $0, f^2(0)$ and $f(0)$. If f is sufficiently close to f_* it cannot be in $(f^2(0), f(0))$ because fI is also a Denjoy interval which is longer than I because the slope of f_* is greater than α_*^2 on $(f_*^2(0), f_*(0))$. But then we have that αI is a Denjoy interval for $\tilde{T}f$. This shows that for all f in some neighbourhood of f_*,

$$I(\tilde{T}(f)) > 0.9|\alpha_*|I(f).$$

This leads to a contradiction since on iteration we get that $I(\tilde{T}^n(f))$ is greater than one for n sufficiently large.

The result now follows because, if f is in the stable manifold and f has a Denjoy interval, then by similar arguments $\tilde{T}^n(f)$ has a Denjoy interval and for large n, $\tilde{T}^n(f)$ will be in the above neighbourhood.

4. The fixed point and its eigenvalues

In this section we discuss the eigenvalues and eigenvectors of the linearisation of the renormalisation transformation T at the two fixed points, and the computation of the strong-coupling fixed point. For clarity we restrict the discussion to the case $\sigma = \sigma_G = (\sqrt{5} - 1)/2$ so that $T = T_1$. All of the ideas presented here generalise immediately to arbitrary rotation numbers with periodic continued fractions.

4.1. *Formal properties of eigenvalues of T*

Let $\Xi_* = (\xi_*, \eta_*)$ denote the strong-coupling fixed point of T. For an appropriate choice of the space of analytic pairs (ξ, η) the derivative of T at Ξ_*, $\mathrm{d}T_* = \mathrm{d}T(\Xi_*)$ is a compact operator [16]. Consequently, its spectrum consists of a countable set of eigenvalues with no accumulation point different from zero. There is no continuous spectrum.

When analyzing the spectrum of $\mathrm{d}T_*$ it is convenient to replace T, which involves a scaling factor which depends upon (ξ, η) by a transformation involving only a constant scaling factor. The price is the introduction of one eigenvalue equal to 1 and some change in the eigenfunctions. To do this we decompose T as

$$T = PC\,, \tag{4.1}$$

where, if $\beta_{\xi,\eta} = \xi(0) - \eta(0)$,

$$P(\xi, \eta)(x) = \beta_{\xi,\eta}^{-1}(\xi, \eta)(\beta_{\xi,\eta}x) \tag{4.2}$$

and

$$C(\xi, \eta)(x) = \alpha_*(\eta, \eta\xi)(x/\alpha_*)$$

where

$$\alpha_* = \frac{1}{\eta_*(0) - \eta_*\xi_*(0)}\,.$$

Since Ξ_* is a fixed point for T and C we have $P(\Xi_*) = \Xi_*$. Also, $P^2 = P$ and

$$PC = PCP. \tag{4.3}$$

Lemma 4.2. The eigenvalues $\lambda \neq 1$ of $\mathrm{d}T_* = \mathrm{d}T(\Xi_*)$ and $\mathrm{d}C_* = \mathrm{d}C(\Xi_*)$ are identical together with their multiplicities. Let $Z_* = (x\xi_*'(x) - \xi_*(x), x\eta_*'(x) - \eta_*(x))$, then it is an eigenvector of $\mathrm{d}C_*$ with eigenvalue 1 but $\mathrm{d}T_* Z_* = 0$.

Remark. We will demonstrate numerically that 1 is not in the spectrum of $\mathrm{d}T_*$ so the restriction to $\lambda \neq 1$ in lemma 4.2 is superfluous.

Proof. The spectrum of $\mathrm{d}P_* = \mathrm{d}P(\Xi^*)$ consists of 0 and 1. The eigenvalue 0 has multiplicity one since its eigenvector $Z = (X, Y)$ satisfies

$$Z = -(X(0) - Y(0))Z_*.$$

We establish the second assertion of the lemma first. Observe that

$$Z_* = \frac{\mathrm{d}}{\mathrm{d}t} s_t(\xi_*, \eta_*)\bigg|_{t=0},$$

where $s_t(\xi, \eta)(x) = (1+t)^{-1}(\xi, \eta)((1+t)x)$. Then

$$Cs_t = s_t \quad \text{and} \quad Ts_t = Ts_0.$$

Differentiating then implies $\mathrm{d}C_* Z_* = Z_*$ and $\mathrm{d}T_* Z_* = 0$.

Now if Z is an eigenvector of $\mathrm{d}C_*$ with eigenvalue λ; then by (4.3) $\mathrm{d}P_* Z$ is an eigenvector of $\mathrm{d}T_*$ and if $\mathrm{d}P_* Z \neq 0$, λ is an eigenvalue. Conversely, if $Z \neq Z_*$ is an eigenvector of $\mathrm{d}T_*$ then so is $\mathrm{d}P_* Z$ and by (4.3)

$$\mathrm{d}C_* Z = Z + cZ_*.$$

But setting $Z = \tilde{Z} + cZ_*/(1-\lambda)$ proves λ is an eigenvalue of $\mathrm{d}C_*$.

Q.E.D.

We now prove a number of results about the eigenvalues of $\mathrm{d}T_*$ and $\mathrm{d}C_*$ which will be useful when we come to interpret the numerical results. Before proceeding we note the following three equalities each of which follows by differentiating the fixed point equations (and the two additional equations obtained by composing the two sides of $\Xi_* = T(\Xi_*)$), three times and utilising $\xi_*'(0) = \xi_*''(0) = 0$:

$$\xi_*'(\eta_*(0)) = \alpha^2, \tag{4.4}$$

$$\eta_*'(\xi_*(0)) = \alpha^4, \tag{4.5}$$

$$\eta_*'(\eta_*\xi_*(0)) = \alpha^2. \tag{4.6}$$

First we consider which eigenvalues can correspond to eigenvectors which are not tangent to the subspace of commuting functions $\xi\eta = \eta\xi$.

Lemma 4.3. If (X, Y) is an eigenvector of $\mathrm{d}C_*$ tangent to $(\xi\eta - \eta\xi)^{(k)}(0) = 0$ for $k < v$ and not tangent to $(\xi\eta - \eta\xi)^{(v)}(0) = 0$ then the associated eigenvalue is $-\alpha^{3-v}$.

Proof. Let $F(\xi, \eta) = \xi\eta - \eta\xi$. Then if $\Xi_* = (\xi_*, \eta_*)$ a simple calculation using $\xi_*\eta_* = \eta_*\xi_*$ shows that

$$\mathrm{d}(F \circ C)(\Xi_*) \cdot (X, Y)(x)$$
$$= -\alpha\eta_*'(\eta_*\xi_*(x/\alpha)) \cdot \mathrm{d}F(\Xi_*) \cdot (X, Y)(x/\alpha).$$

But by (4.6) $\eta_*'(\eta_*\xi_*(0)) = \alpha^2$ so the result follows by differentiating both sides v times at 0.

Q.E.D.

Note that lemma 4.3 tells us that any eigenvector whose eigenvalue is not a power of α is tangent to the commuting subspace.

We now consider eigenvectors which are not analytic functions of x^3.

Lemma 4.4. If (X, Y) is an eigenvector of $\mathrm{d}C_*$ on $\mathrm{d}T_*$, then either X and Y are analytic functions of x^3 or the associated eigenvalue is $\lambda = \pm\alpha^{3-p}$ where p is the least integer which is not a multiple of 3 such that the pth-derivative $X^{(p)}(0) \neq 0$. In the latter case the sign of λ is $(-)^{p+1}$ sign $(X^{(p)}(0)\cdot Y^{(p)}(0))$.

Proof. By the lemma 4.2 we need only prove this for C. Let (X, Y) be an eigenvector which is not a function of x^3 and let p be as above. If λ is the eigenvalue,

$$\lambda X(x) = \alpha Y(x/\alpha)\,, \tag{4.7a}$$

$$\lambda Y(x) = \alpha\eta'_*(\xi_*(x/\alpha))\cdot X(x/\alpha) + \alpha Y(\xi_*(x/\alpha))\,. \tag{4.7b}$$

In (4.7b) the terms $\alpha Y(\xi_*(x/\alpha))$ and $\alpha\eta'(\xi_*(x/\alpha))$ are analytic functions of x^3 since ξ_* is. Consequently, we deduce that

$$\lambda Y^{(p)}(0) = \alpha^{1-p}\eta'_*(\xi_*(0))X^{(p)}(0)\,. \tag{4.8}$$

Thus differentiating (4.7a) p times at 0 and substituting in (4.8) we obtain

$$\lambda^2 = \eta'_*(\xi_*(0))\alpha^{2-2p}\,.$$

But $\eta'_*(\xi_*(0)) = \alpha^4$ by (4.5). Q.E.D.

Of particular interest is the amount by which a small linear term added to the fixed point is amplified by iteration of the renormalisation transformation. This describes the "cross-over" from critical maps to diffeomorphisms. Later, we will obtain information about the structure of conjugacies from our knowledge of this "cross-over".

Lemma 4.5. If (X, Y) is an eigenvector of $\mathrm{d}C_*$ or $\mathrm{d}T_*$ tangent to $(\xi\eta - \xi\eta)'(0) = 0$ and such that $X(0) = Y(0)$ but $X'(0) \neq 0$ or $Y'(0) \neq 0$ then the associated eigenvalue is $\gamma = \alpha^2$ and $\mathrm{sign}(X'(0)) = \mathrm{sign}(Y'(0))$.

Remark. We will later give evidence for the existence of such an eigenvector.

Proof. By lemma 4.4, $\gamma = \pm\alpha^2$. By combining the linear equation obtained from the condition that (X, Y) is tangent to $(\xi\eta - \eta\xi)'(0) = 0$ with

$$\mathrm{d}C_*\cdot(X, Y) = \lambda(X, Y)$$

we obtain

$$Y'(0)[\xi'_*(\eta_*(0)) - \lambda] = 0$$

and $Y'(0) \neq 0$. Therefore $\lambda = \xi'_*(\eta_*(0)) = \alpha^2$. Q.E.D.

Finally, we note that if we let

$$s_t(\xi, \eta) = (\mathbb{1} + t\sigma)^{-1}\circ(\xi, \eta)\circ(\mathbb{1} + t\sigma)\,,$$

then

$$Z(\sigma) = \frac{\mathrm{d}}{\mathrm{d}t}s_t(\xi_*, \eta_*) = (\xi'_*\sigma - \sigma\xi_*, \eta_*\sigma - \sigma\eta_*)$$

is an eigenvector of $\mathrm{d}C(\xi_*, \eta_*)$ if

$$\alpha\sigma(x/\alpha) \equiv \lambda\sigma(x) \tag{4.9}$$

and then the associated eigenvalue is λ. In particular, the coordinate changes corresponding to $\sigma(x) = x^n$ give eigenvectors of $\mathrm{d}C$ with eigenvalue $\lambda = \alpha^{1-n}$. The only eigenvalues λ with $|\lambda| \geqslant 1$ produced in this way correspond to $n = 0$ and 1, i.e., to a shift of origin and a change of scale. Recall that the eigenvector for the latter lies in the kernel of $\mathrm{d}P_*$ and therefore yields an eigenvalue of 0 for $\mathrm{d}T_*$ (lemma 4.2).

4.2. *Calculation of fixed points*

We now describe how the strong-coupling fixed point (ξ_*, η_*) of our renormalisation transformation T was obtained numerically. We mainly deal here with the case where $T = T_1$ so that $\sigma = \sigma_G$. It will be clear how to generalise the procedure so as to treat $\sigma = \rho(f)$ with an arbitrary periodic continued fraction.

Because of the nonlinear nature of $\mathscr{S}$ and S_{crit} it is numerically convenient to relax the conditions

3.3(b) and (g), extend T to the bigger space and then remove those eigenfunctions which violate these conditions. In lemma 3.2 we proved that the strong coupling fixed point (ξ_*, η_*) is an analytic function of x^3 if it exists. We therefore only consider the action of T on the subspace consisting of those (ξ, η) which are analytic functions of x^3. This subspace is invariant under T. We approximate (ξ, η) by

$$\xi(x) = \sum_{n=0}^{N-1} a_n x^{3n} ,$$

$$\eta(x) = \sum_{n=0}^{N-1} b_n x^{3n} .$$

For a fixed N we can define on the space $\mathbb{R}^{2N}$ of coefficients a_i, b_i an approximation, $\hat{T}$, to T by means of the following equations:

$$\sum_{n=0}^{N-1} a_n (x_m^{\mathrm{R}})^{3n} = \alpha\eta(x_m^{\mathrm{R}}/\alpha) , \qquad (4.10a)$$

$$\sum_{n=0}^{N-1} b_n (x_m^{\mathrm{L}})^{3n} = \alpha\eta\xi(x_m^{\mathrm{L}}/\alpha) , \qquad (4.10b)$$

where

$$1 \leqslant m \leqslant N ,$$

$$x_m^{\mathrm{R}} = \left(\frac{m-1}{N-1}\right)^{1/3} \alpha\eta(\xi(0)) ,$$

$$x_m^{\mathrm{L}} = \left(\frac{m-1}{N-1}\right)^{1/3} \alpha\eta(0) ,$$

and

$$\alpha^{-1} = \eta(0) - \eta\xi(0) . \qquad (4.10c)$$

The idea of distributing the matching points x_m^{R}, x_m^{L} in this way is due to Feigenbaum [11]. Now both α and the righthand side of (4.10b) are nonlinear functions of the coefficients a_i, b_i from the last approximation to (ξ, η). Inversion of the coefficient matrix formed by the powers of x^{L}, x^{R} on the left-hand side of (4.10) yields the new (a_i, b_i) and completes the definition of T.

Newton's method may then be applied to find a fixed point of this nonlinear system. With 14-figure numerical accuracy the convergence ceased to improve for N beyond 11 and ultimately Newton's method would not converge. For $N = 11$ however the fixed point equation is satisfied to within 10^{-7} over the entire interval. The series for (ξ, η) however does not appear to converge over the entire interval since the contribution of the last term at the boundary is only a factor of 10 smaller than the first few terms. We suspect that there are singularities of (ξ, η) in the complex plane that determine the radius of convergence of a Taylor series and some other expansion point than 0 should be used [21]. However, since we can accurately approximate a solution of the fixed point equations in the space (a_i, b_i) we can also compute the relevant eigenvalues of $\mathrm{d}T_*$ with comparable accuracy.

The differentiation $\mathrm{d}T(a_*, b_*)$ was done numerically. (It is as easy to compute $\mathrm{d}C(a_*, b_*)$ by omitting eq. (4.10c) and fixing α at its fixed point value.) For $N = 11$ we find three eigenvalues λ with $|\lambda| \gtrsim 1$;

$$\delta = -2.83362 \pm 2 \times 10^{-5} = -\sigma_{\mathrm{G}}^{-2.16444} ,$$

$$\lambda_1 = 2.1395796 ,$$

$$\lambda_2 = -0.99997 ,$$

while from the fixed point calculation

$$\alpha = -1.288575 \pm 15 \times 10^{-6} = -\sigma_{\mathrm{G}}^{-0.5268718} .$$

The error bars on α and δ are somewhat subjective and based on comparison between the approximations for various N.

We believe that λ_1 and λ_2 actually equal $-\alpha^3$ $(=2.139583)$ and -1. These are expected by lemma 4.3 since we have not imposed the conditions $(\xi\eta - \eta\xi)^{(\nu)}(0) = 0$ for $\nu = 0, 3$ on the eigenvectors and indeed we find numerically that the eigenvectors associated with $\lambda_{1,2}$ violate their respective conditions by an amount of order 1. The agreement between $\lambda_{1,2}$ and $-\alpha^3$, -1 is an additional check on the quality of our numerics. We also infer (and verified) that since δ is not a power of α, lemma 4.3 implies it must be tangent to $\xi\eta(x) \equiv \eta\xi(x)$.

The leading irrelevant eigenvalue (in $\mathscr{S}_{\text{crit}}$) is determined to far less accuracy and we estimate

$$|\lambda_3| = 0.52 \pm 0.02\,.$$

We therefore conclude this: The spectrum of $\mathrm{d}T(\xi_*, \eta_*)$ restricted to the tangent space of $\mathscr{S}_{\text{crit}}$ consists of an eigenvalue $\delta = 2.83362$ and a countable number of eigenvalues λ such that $|\lambda| < 0.54$.

Let R denote the set of those (ξ, η) in $\mathscr{S}_{\text{crit}}$ such that $\rho(\xi, \eta) = \sigma_{\text{G}}$. It is clear that the stable manifold of (ξ_*, η_*) in $\mathscr{S}_{\text{crit}}$ is contained in R. We shall assume that near (ξ_*, η_*), R is contained in the stable manifold. (Merely knowing the eigenvalue spectrum of $\mathrm{d}T$ is not sufficient to exclude the possibility that there are small regions of the R manifold close to the fixed point but not in the stable manifold. This is known not to occur for maps with an ϵ-singularity for $\epsilon \geqslant 0$ small.

Then we deduce that *the eigenspace associated with δ is transverse to R*. This is because R is of co-dimension one in $\mathscr{S}_{\text{crit}}$ and the compact operator $\mathrm{d}T_*$ leaves invariant its tangent space. Consequently, there is a one-dimensional subspace complementary to the tangent space of R which is invariant under $\mathrm{d}T_*$. Clearly, this must be the eigenspace corresponding to δ.

With some mild assumptions on the nature of the sets $\rho = p_n/q_n$ (see ref. 16) it now follows (by an argument similar to that given by Collet, Eckmann and Lanford [17]) that if (ξ_μ, η_μ) is a one-parameter family in $\mathscr{S}_{\text{crit}}$ which is transverse to R and if μ_k is such that 0 is a periodic point with rotation number p_k/q_k of the circle map defined by $(\xi_{\mu_k}, \eta_{\mu_k})$ then

$$\lim_{j\to\infty} \delta^j(\mu_j - \lim_{k\to\infty} \mu_k) \tag{4.11}$$

exists and is non-zero.

We now argue that $\mathrm{d}T_* = \mathrm{d}T(\xi_*, \eta_*)$ has one other eigenvector γ which is transverse to $\mathscr{S}_{\text{crit}}$, tangent to $\rho = \sigma_{\text{G}}$ and has an eigenvalue $= \alpha^2$. We know from general principles [22] and find from numerical experiments that (ξ_*, η_*) is not attracting under T restricted to $\rho = \sigma_{\text{G}}$. For example, we find if $f_a(\theta) = \theta + \omega_* - (a/2\pi)\sin 2\pi\theta$ with ω_* chosen so that $\rho(f_a) = \sigma_{\text{G}}$, then $T^n(f_{1-(\epsilon/\alpha^{2n})})$ converges as $n \to \infty$ to a function near (ξ_*, η_*) (see section 5). Also by the results described above we know that $\mathrm{d}T_*$ has no eigenvalue λ with $|\lambda| = 1$. Thus $\mathrm{d}T_*$ must have an eigenvector transverse to $\mathscr{S}_{\text{crit}}$ in $\mathscr{S}$ with an eigenvalue γ such that $|\gamma| > 1$. By lemma 4.4 one must then have that $\gamma = \pm\alpha^{3-p}$ where $p = 1, 2$. The case $p = 2$ is not possible, for then the eigenvector is not tangent to $\xi''(0) = 0 = \eta''(0)$. Thus we deduce that $p = 1$. Then it follows from lemma 4.5 that $\gamma = \alpha^2$.

The same numerical procedures have been implemented for the case where the rotation number $\sigma = (\sqrt{2} - 1) = [2, 2, 2, \ldots]$. Again, in the space of functions analytic in x^3, we obtain for $N = 8$ three eigenvalues λ with $|\lambda| \gtrsim 1$:

$$\delta = -6.79924 \pm 2 \times 10^{-5} = -\sigma^{-0.17480}\,,$$

$$\lambda_1 = 3.99563\,,$$

$$\lambda_2 = -0.9999989\,,$$

and from the fixed point

$$\alpha = 1.586822 \pm 2 \times 10^{-6} = \sigma^{-0.523879}$$

we again infer that $\lambda_1 = \alpha^3 = 3.99562$ and $\lambda_2 = -1$.

By relaxing condition 3.3(f), a number of numerical experiments were done in which T_1 was applied to a cubic critical map with the inflection point not at the origin. No fixed point was found and the position of the inflection point moved randomly around the unit interval.

4.3. *Eigenvalues at the weak-coupling fixed point*

The weak-coupling fixed point for $T = T_1$ is given by

$$(\xi_*, \eta_*)(x) = (x + \sigma_G, x - \sigma_G^2),$$

and the associated value of α is $-1/\sigma_G$. For the rest of this section we will work with C rather than T. If (X, Y) is an eigenvector of dC_* then

$$\lambda Y(x) = \alpha Y(\xi_*(x/\alpha)) + (\alpha^2/\lambda) Y(x/\alpha^2).$$

Therefore, if we take $Y(x) = \Sigma_{n=0}^N a_n x^n$ we find that

$$\lambda = \alpha^{-N} \quad \text{or} \quad -\alpha^{2-N}.$$

There are thus four eigenvalues λ of dC_* with $|\lambda| \geqslant 1$ namely ± 1, $-\alpha$ and $-\alpha^2$. The associated eigenvectors are

$$e_{-1} = (-\tfrac{1}{2}\alpha^{-1} - 2\alpha^{-1}x - \alpha^{-1}x^2, \ \tfrac{1}{2}\alpha^{-2} + 2\alpha^{-1}x + x^2),$$

$$e_1 = (\alpha, 1),$$

$$e_{-\alpha^2} = (-\alpha^{-1}, 1),$$

and

$$e_{-\alpha} = (-\alpha^{-1} - \alpha^{-1}x, \quad \alpha^{-1} + x).$$

The eigenvector e_1 is an infinitesimal scale transform and is not an eigenvector of dT_*. Also $e_{-\alpha}$ and e_{-1} respectively are not tangent to $\xi\eta(0) = \eta\xi(0)$ and $(\xi\eta - \eta\xi)'(0) = 0$.

Thus the only eigenvalue λ of dT_* with $|\lambda| > 1$ is $\delta = -\alpha^2 = -1/\sigma_G^2$. The eigenvector of dT_* corresponding to $e_{-\alpha^2}$ is tangent to the curve $\mu \to (\xi_* + \mu, \eta_* + \mu)$ which is the unstable manifold of the weak coupling fixed point.

5. Coordinate changes and conjugacies

5.1. *Definitions and basic ideas*

In 3.4 we showed that all functions on the stable manifold of the cubic critical map with rotation number σ_G are conjugate to R_{σ_G}. We now consider in detail the structure of the homeomorphism h which conjugates a cubic critical map f with irrational rotation number σ to the rotation R_σ, i.e., $h^{-1}fh = R_\sigma$. Note that if h is known, then time-series can be reconstructed because $f^m(x) = h(h^{-1}x + m\sigma)$. It will be important to extend the notion of such a conjugacy to deal with the function pairs of our renormalisation group.

Definition. Let $(\xi, \eta) \in \mathscr{S}_n$ be such that $\rho(\xi, \eta) = \sigma$. A *conjugating homeomorphism* of (ξ, η) is a homeomorphism $h: (\sigma - 1, \sigma] \to (\eta(0), \xi(0)]$ such that $h(0) = 0$ and

$$\begin{aligned} \xi h(x) &= h(x + \sigma), \quad \sigma - 1 < x \leqslant 0, \\ \eta h(x) &= h(x + \sigma - 1), \quad 0 < x \leqslant \sigma. \end{aligned} \tag{5.1}$$

To be consistent with (5.1) we define R_σ on $(\sigma - 1, \sigma)$ by

$$R_\sigma(x) = \begin{cases} x + \sigma, & \sigma - 1 < x \leqslant 0, \\ x + \sigma - 1, & 0 < x \leqslant \sigma. \end{cases}$$

Note that if $f_{\xi,\eta}$ is the associated circle homeomorphism then h conjugates $f_{\xi,\eta}$ to the rotation R_σ in the usual sense. If h exists it is unique. When we wish to stress the dependence of h upon (ξ, η) or $f = f_{\xi,\eta}$ we will write it $h_{(\xi,\eta)}$ or h_f.

The conjugating homeomorphism transforms under the renormalisation transformation in a particularly simple way. If $\Xi = (\xi, \eta) \in \mathscr{S}_n$, a straightforward calculation gives

$$h_{T_n(\Xi)}(\theta) = \alpha h_\Xi(-\sigma\theta), \tag{5.2}$$

where as before $\alpha = 1/(\xi^{n-1}\eta(0) - \xi^n\eta(0))$.

Fig. 6 shows h for $\rho = \sigma_G$ and the critical map (2.7). The curve is nowhere continuously differentiable since by its definition when f has a critical point at the origin, h must have zero derivative at σ_G and/or an infinite derivative at 0. Numerically both singularities are present, and the action of f then creates points of zero derivative at

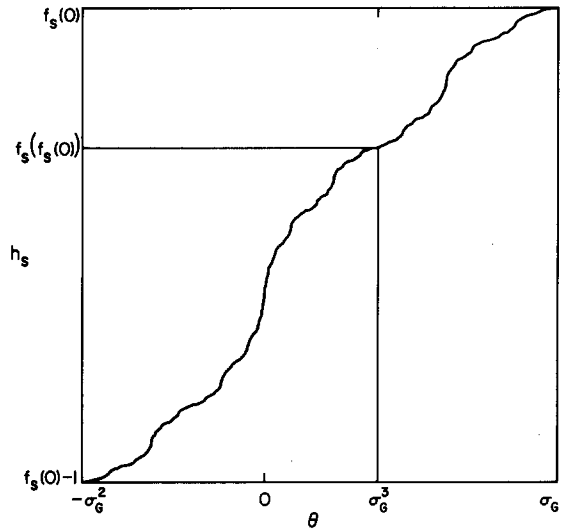

Fig. 6. The conjugate homeomorphism h_s for the sine map (5.4) with $a = 1$ and $\rho = \sigma_G$. Note the points of infinite slope at $\theta = n\sigma_G$ (mod 1), $n \leqslant 0$ and of zero slope at $n\sigma_G$ (mod 1), $n > 0$. Under the scaling (5.2), the region in the box may be inverted and expanded to fill the entire figure. Note by (5.2), the homeomorphism h_* for the fixed point f_* satisfies $h_*(-(-\sigma_G)^n) = \alpha^{2-n}/(\alpha - 1)$.

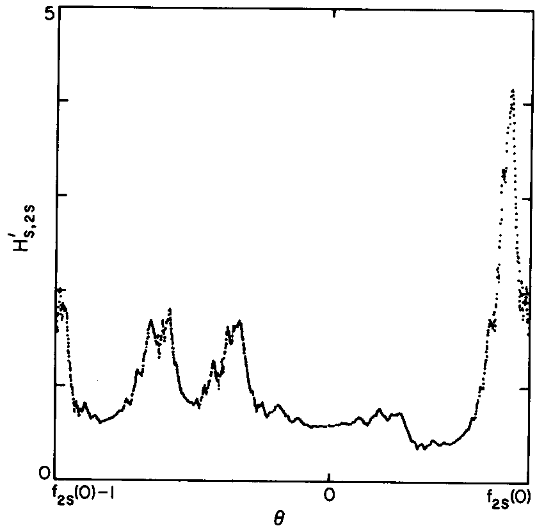

Fig. 7. The first derivative of the homeomorphism $H_{s,2s}$ linking the sine map f_s (5.4) and $a = 1$ with the map $f_{2s}(\theta) = \theta + \omega' - a/8\pi(\sin(2\pi\theta) + \sin(6\pi\theta))$ on the critical surface ($a = 1$). The winding number of both maps has a random bounded continued fraction, (2, 2, 1, 1, 2, 1, 1, 2, 1, 1, 1, 1, 2, 2, 2, . . .) based on the binary expansion of π. The first derivative appears continuous but the second derivative is nowhere continuous if it exists at all. The corresponding graph for a periodic winding number (e.g., σ_G) would be similar (conjecture A).

$n_1\sigma - n_2$, $n_1 > 0$ while f^{-1} does the same; creating singularities at $n_1\sigma - n_2$, $n_1 \leqslant 0$.

If $\Xi = (\xi, \eta)$ and $\Xi' = (\xi', \eta')$ have conjugate homeomorphisms h_Ξ and $h_{\Xi'}$ we denote $h_\Xi \circ h_{\Xi'}^{-1}$, by $H_{\Xi,\Xi'}$. Then $H_{\Xi,\Xi'}$ is a homeomorphism linking Ξ to Ξ'; in particular if $H = H_{\Xi,\Xi'}$,

$$H^{-1} f_\Xi H = f_{\Xi'} .$$

By (5.2),

$$H_{T_n(\Xi), T_n(\Xi')}(\theta) = \alpha(\Xi) H_{\Xi,\Xi'}(\alpha(\Xi')^{-1}\theta) . \tag{5.3}$$

If $f = f_\Xi$ and $g = f_{\Xi'}$, then we shall often denote $H_{\Xi,\Xi'}$ by $H_{f,g}$. We shall be particularly interested in the case where $\Xi' = T_n(\Xi)$ and then we call H the *incremental homeomorphism*.

Clearly if f is a cubic critical map and g a diffeomorphism with $\rho(g) = \rho(f)$ then $H_{f,g}$, if it exists, is nowhere differentiable because f^{-1} is not differentiable. On the other hand, we have numerical evidence that there is a continuously differentiable homeomorphism conjugating two cubic critical maps whose rotation number has bounded entries in its continued fraction. The first derivative (fig. 7) was computed from a cubic spline fit to the numerical data and appears well-resolved and continuous. However, the same numerics indicate that this conjugacy is not twice continuously differentiable and in addition its Fourier transform falls off as $1/n^2$ over three decades. On this evidence we make the following conjecture.

Conjecture A. Let f and g be generic critical maps of the circle with $\rho(f) = \rho(g)$ in Herman's set [13] A. Then there is a once continuously differentiable diffeomorphism H such that $H^{-1}fH = g$.

As it stands this conjecture does not cover the circle homeomorphism $f = f_{\xi,\eta}$ obtained from our renormalisation group because this has discontinuities in its derivatives at 0 and $f(0)$. However, our numerical results indicated that it can be

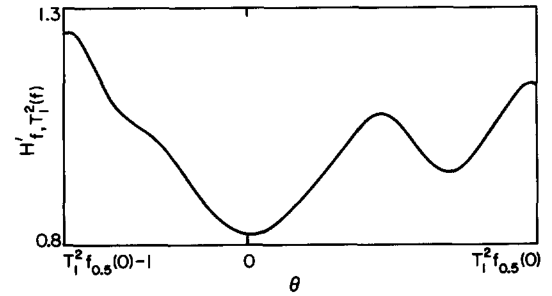

Fig. 8. First derivative of the homeomorphism linking the sine map for $a = 0.5$ (5.4) with T_1^2 acting on the same map. The rotation number is σ_G and the only singularity appears to be a jump discontinuity at the boundary. Three additional derivatives were shown to exist numerically as they must.

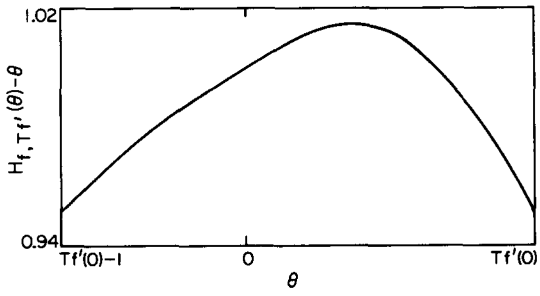

Fig. 9. Periodic part of the homeomorphism linking the sine map, f, for $a = 1 - \alpha^{-n}$ to T_1 acting on the sine map, f', for $a = 1 - \alpha^{-(n+2)}$, $n = 20$. f and $T_1 f'$ are close and approximately equidistant to the critical surface, H would appear unchanged to the eye if we let $n \to \infty$. The first derivative of H is similar to fig. 7 except for a discontinuity at the boundary (conjecture B).

extended with the following qualification: from (5.3) it is clear that the discontinuities introduced by $T = T_n$ force a discontinuity of the first derivative of $H_{\tilde{T}f,\tilde{T}g}$ at $\tilde{T}g(0)$, but leave H with left and right derivatives at that point. With this qualification, figs. 8 and 9 provide evidence that H remains smooth over the range of T.

Let f_a be the map in the family

$$f_{\omega,a}(\theta) = \theta + \omega - (a/2\pi)\sin 2\pi\theta \tag{5.4}$$

which is such that $\rho(f_{a,\omega(a)}) = \sigma_G$. (We shall often refer to eq. (5.4) as the *sine map*.) Fig. 8 shows the first derivative of the iterated homeomorphism H_{f,T^2f} when $f = f_{1/2}$. The numerical evidence indicates that it has at least four continuous derivatives, except for the first derivative discontinuity at the boundary.

Fig. 9 is visually indistinguishable from the incremental homeomorphism $H_f = H_{f,Tf}$ for the cubic critical map $f = f_1$. This homeomorphism remains continuously differentiable, but the second derivative has singularities (apparently at images of the critical point 0).

Note that to study the smoothness of the maps $H_{f,g}$ it suffices to consider the case where g is an analytic map. This is because if the only discontinuities in the derivatives of $H_{e,g}$ and $H_{f,g}$ are at $g(0)$ then $H_{e,f} = H_{e,g} \circ H_{f,g}^{-1}$ is smooth except at $f(0)$: thus instead of $H_{e,f}$ we can study $H_{e,g}$ and $H_{f,g}$ and choose g to be analytic. Let $(\xi,\eta) \in \mathscr{S}_{\text{crit}}$ and suppose that (ξ,η) can be conjugated to a cubic critical map g, i.e., $H^{-1}\xi H = g$ and $H^{-1}\eta H = g - 1$ where H is continuously differentiable except at $g(0) = y = x + 1$ where one-sided derivatives exist. Then $(H^{-1}\eta)'''(0) = (H^{-1}\xi)'''(0)$, $(\eta H)'(y) = (\xi H)'(x)$, which together imply $(\eta\xi)'''(0) = (\xi\eta)'''(0)$. Since some degree of connectivity between (ξ,η) is necessary for H to have the observed smoothness, we conjecture $\xi\eta = \eta\xi$ is in fact sufficient.

Conjecture B. If $\Xi_1 = (\xi_1,\eta_1)$ and $\Xi_2 = (\xi_2,\eta_2)$ are in $\mathscr{S}_{\text{crit}}$, $\xi_i\eta_i = \eta_i\xi_i$ for $i = 1, 2$ and $\rho(\Xi_1) = \rho(\Xi_2) = \sigma \in A$ then the homeomorphism $H = H_{\Xi_1,\Xi_2}$ exists and it and its inverse are once continuously differentiable except at the end-points $\eta_i(0)$ and $\xi_i(0)$.

Note that the (ξ,η) such that $\xi\eta = \eta\xi$ are the only physically important ones.

Suppose now that f is an analytic diffeomorphism with $\rho(f) \in A$. Then the conjugating diffeomorphism exists and is analytic by Hermans' theorem [7]. Consequently, we can use (5.2) to construct conjugating homeomorphisms for all the images of $(f, f-1)$ under the renormalisation transformation. Clearly, by (5.2) this conjugacy is analytic except at the boundary and has an inverse with this property. The incremental homeomorphism between any two images can then be factored through the simple rotations. One thereby established a stronger form of conjecture B for diffeomorphisms.

The universal features in the transition we study should not depend upon the particular choice of coordinates used to describe the system, i.e., they should be invariant under smooth changes of coordinates. This is particularly relevant for experiments for there one usually has no control over the coordinate system in which data is presented. In this context we will invoke the conjectures of this section when we discuss the universal features of an experimental spectrum. Because we allow arbitrary smooth coordinate changes, universal features must reflect some singular property of the physical process. Precisely how to factor out the non-singular non-universal content from real experimental data is discussed in section 6.

For the remainder of this section we shall confine the discussion to maps with rotation number $\rho = \sigma_G = (\sqrt{5} - 1)/2$; the results apply mutatis mutandis to all rotation numbers with periodic continued fractions.

Recall the nature of the renormalisation transformation T near the strong-coupling fixed point $f_* = (\xi_*, \eta_*)$ (section 3). The fixed points has a two-dimensional unstable manifold U and a codimension two stable manifold $\mathscr{S}$. One eigendirection in U corresponds to the eigenvalue δ; the other is tangent to the curve Σ of (ξ, η) in U with rotation number σ_G. The associated eigenvalue is $\gamma = \alpha^2$ (see section 4).

Now consider a one-parameter family $f_{1-\epsilon}$ of maps which crosses $\mathscr{S}_{\text{crit}}$ transversally at $\epsilon = 0$ and such that $\rho(f_{1-\epsilon}) = \sigma_G$. Then the numerical evidence is that the derivative homeomorphism conjugating $f_{1-\epsilon}$ to $T_1(f_{1-\epsilon\gamma^{-1}})$ is continuous in both x (boundaries excluded) and ϵ as $\epsilon \to 0$ (fig. 9). For $\epsilon = 0$ this amounts to conjecture B. Furthermore, $T^n(f_{1-\epsilon\gamma^{-n}})$ converges for fixed ϵ to a point on Σ. (Numerically, for $n = 1, \dots, 6$ and $\epsilon = 0.05$ the convergence is comparable to that on the critical surface $\mathscr{S}_{\text{crit}}$.) Thus for diffeomorphisms f and f_* one can decompose the conjugate homeomorphism into a "horizontal" part that conjugates f to a point on Σ, and a universal "vertical" part linking the latter to R_{σ_G}.

Let f_a, $a = 1 - \epsilon$, be a one-parameter family as above. Let h_a conjugate f_a to R_{σ_G}. As $a \to 1$, h_a develops structure on finer and finer length scales. The length scale as a function of a can be estimated using our renormalisation transformation. It will take $n_a \approx -\log(1-a)/\log(\alpha^2)$ iterations of T to relate f_a to a map whose first derivative at the origin is of order one. Since each application of T_1 expands the scale of h_a by σ_G^{-1}, h_a has structure on all length scales down to $\sigma_G^{n_a} = (1-a)^s$ where $s = -\log(\sigma_G)/\log(\alpha^2)$.

Finally, we pose the problem of whether one can use Σ to understand more about the structure of the fixed point f_*. For example, what can we learn by decomposing the conjugate homeomorphism h_{f_*} of f_* into a series of incremental homeomorphisms

$$h_{f_*} = \cdots \circ H_{f_n, f_{n+1}} \circ H_{f_{n+1}, f_{n+2}} \circ \cdots,$$

with $f_n \in \Sigma$, $f_{n+1} = Tf_n$, $f_n \to f_*$ as $n \to -\infty$ and $f_n \to R_{\sigma_G}$ as $n \to +\infty$? This seems quite in the spirit of K.A.M. theory. Unfortunately, the incremental homeomorphisms themselves become complicated near f_* (fig. 10).

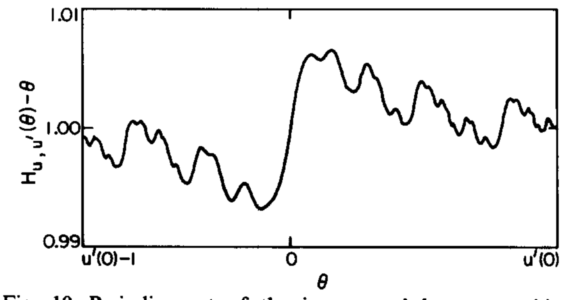

Fig. 10. Periodic part of the incremental homeomorphism linking pairs of maps (u, u') along the unstable manifold of the nonlinear fixed point for $\rho = \sigma_G$. We have approximated $u_\epsilon = \lim_{n\to\infty} T_1^n(f_{a=1-\epsilon/\alpha^{2n}})$ by taking $n = 5$ and f to be the sine map. The figure then compares $u = u_\epsilon$ to $u' = \mu_{\epsilon/\alpha^2}$ for $\epsilon = \alpha^{-12}$. As $\epsilon \to 0$ the oscillations in $H_{u,u'}$ increase in number without decreasing in relative amplitude.

6. Universal scaling structure of spectra

Perhaps the most striking feature of the transition we study is the Fourier spectrum. Fig. 11 shows the power spectrum $|\tilde{f}_s(\omega)|^2$ for a time series found by iterating the sine map (5.4) with winding number equal to σ_G. The low frequency peaks in the spectrum are universal and self-similar. For good winding numbers (i.e., in A) [13] with aperiodic continued fractions the spectrum no longer is self-similar, but has structure on all time scales (fig. 12). The low frequency behavior remains universal. More precisely, the fractional difference in the spectra for two different maps with the same winding number is proportional to ω as $\omega \to 0$ (fig. 13).

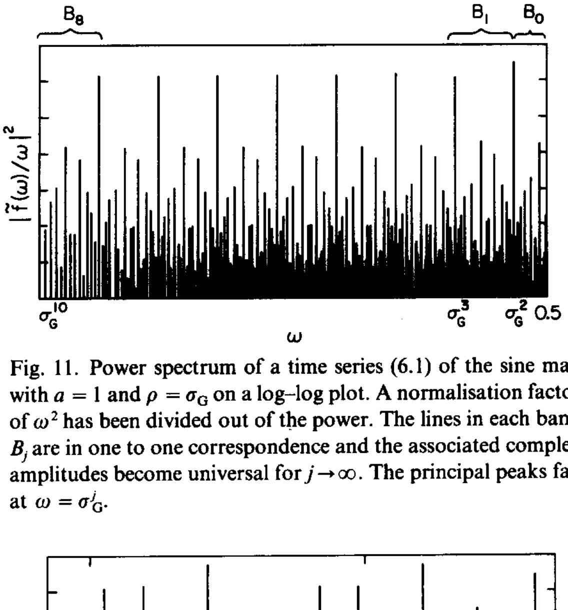

Fig. 11. Power spectrum of a time series (6.1) of the sine map with $a = 1$ and $\rho = \sigma_G$ on a log–log plot. A normalisation factor of ω^2 has been divided out of the power. The lines in each band B_j are in one to one correspondence and the associated complex amplitudes become universal for $j \to \infty$. The principal peaks fall at $\omega = \sigma_G^j$.

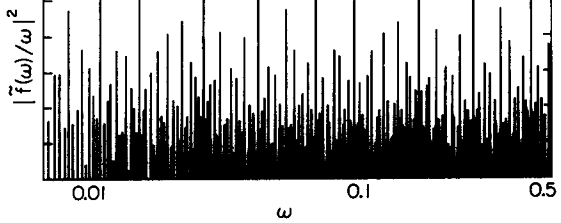

Fig. 12. Power spectrum of the sine map at $a = 1$ as in fig. 11 except now the rotation number is the one of fig. 7 and does not have a periodic continued fraction. The low frequency spectrum is universal but not self-similar.

We have argued above and will further justify in section 8 that the universal features associated with those transitions involving the explosion of an irrational torus are embodied in those of cubic critical maps of the circle. There are, however, some practical considerations involved in comparing an experimental system with a circle map. This section begins with a discussion of these experimental issues.

The rest of the section analyzes the scaling and universality of the spectrum. We prove a lemma bounding the low frequency spectrum for good winding numbers. We give numerical evidence for a conjecture about the behavior of the low frequency spectrum under coordinate changes. We use these results and the conjectures of the previous section to explain the low frequency spectral universality for all good winding numbers. We also use these results to show for winding numbers with periodic continued fractions that the low frequency spectrum is self-similar. We study this by reducing the scaling law for the spectrum of the fixed point map to that of a linear system.

6.1. *General remarks*

In the quasi-periodic regime one chooses two base frequencies ω_1 and ω_2, the Fourier peaks then lie at $n\omega_1 + m\omega_2$, $n, m \in \mathbb{Z}$. We claim that the universal features of the transition depend upon $\rho = \omega_1/\omega_2$. Now, there is some ambiguity in the choice of the base frequencies; if q, r, s and t are integers with $qt - rs = \pm 1$, then one could equally well choose the frequencies $q\omega_1 + r\omega_2$, $s\omega_1 + t\omega_2$ to label the peaks. Clearly, the universal properties of the transitions associated with $\rho' = (q\omega_1 + r\omega_2)/(s\omega_1 + t\omega_2)$ should be the same as for ρ. One can see this from our renormalisation group by utilising the following result:

Lemma 6.1. Let the continued fraction expansion of ρ be $[k_1, k_2, \ldots]$ and that of ρ' be $[l_1, l_2, \ldots]$. Then some tail $(k_n, k_{n+1}, \ldots)$ of ρ equals a tail $(l_m, l_{m+1}, \ldots)$ of ρ' if and only if $\rho' = (q\rho + r)/(s\rho + t)$ for $|qt - rs| = 1$ all integers.

Proof. The property of "having the same tail" is clearly an equivalence relation; we shall write $\sigma \sim \sigma'$ if σ and σ' have the same tail. So also is the property of "being related by an integral linear fractional transformation of determinant ± 1"; compositions of such transformations are given by the products of the corresponding matrices. We shall $\sigma \sim \sigma'$ if σ' can be written as a ratio $(q\sigma + r)/(s\sigma + t)$ with $|qt - rs| = 1$ all integers.

First, $\rho \sim (-k_1\rho + 1)/(\rho + 0) = (k_2, k_3, \ldots)$; by induction if $\rho \sim \rho'$ then $\rho \sim \rho'$. Conversely, suppose $\rho \sim \rho'$. It is easily shown that $\sigma \sim \sigma^{-1} \sim \sigma - n \sim -\sigma$ for $n \in \mathbb{Z}$ under both $\sim$ and $\sim$. We shall use a sequence of these transformation to construct a ρ^* satisfying $\rho' \sim \rho^* \sim \rho$. Starting with $\rho_0^* = \rho'$, we know $\rho' \sim \rho_0^* \sim \rho$; Let $\rho_n^* = (q_n\rho + r_n)/(s_n\rho + t_n)$; if $s_n \neq 0$, by subtracting the nearest integer to q_n/s_n from ρ^* we may assume always that $|q_n| < |s_n|$. Let $\rho_{n+1}^* = 1/\rho_n$ minus the integer part; then $|s_{n+1}| = |q_n| < |s_n|$. After at most s_0 steps $s = 0$. But then $qt = \pm 1$, and we know $\rho' \sim \rho^* = (\pm\rho + r)/(0\rho \pm 1) \sim \rho$.

Q.E.D.

In each application of our RG transformation, one integer in the continued fraction expansion of the winding number is removed (lemma 3.1). The universal features depend only upon the tail of the continued fraction for ρ; the initial integers are irrelevant. The above lemma demonstrates that this formal irrelevance is an experimental ambiguity; it is a consistency check for our theory.

6.2. *Scaling theory for spectra*

The arguments in the section proceed as follows:

1) Using the conjectures of section 5 and conjecture C below we conclude for winding numbers in A [13] that the behaviour of the low-frequency spectrum is independent of the mapping, i.e., universal. Thus for periodic winding numbers it suffices to consider how the spectrum of the fixed point function scales.

2) We show that for a certain piecewise-linear fixed point for $\sigma = \sigma_G$ the spectrum is self similar and scales as ω as $\omega \to 0$.

3) We then show using 2 and conjecture C, that the true fixed point f_* for $\sigma = \sigma_G$ satisfies the same scaling relation.

Consider a Poincaré map obtained from a cross-section of a flow on an attracting invariant torus. In the quasi-periodic regime if we adjust our units to make $\omega_2 = 1$ then the experimental spectrum will have peaks at $-\frac{1}{2} < \omega = n\sigma + m < \frac{1}{2}$ where $\sigma = \rho(f)$ is the rotation number of the map and n and m are integers. Of course, experiments will measure only observables which are periodic functions of the angular variable θ.

We shall specifically consider the observable $f^n(\theta) - R_\sigma^n(\theta)$. Its power spectrum $|\tilde{f}(\omega)|^2$ is given by

$$\tilde{f}(\omega) = \lim_{L\to\infty} \frac{1}{L} \sum_{l=0}^{L-1} \exp(2\pi i l\omega)(f^l(0) - R_\sigma^l(0)), \quad (6.1)$$

a form which is very convenient analytically. For numerical or experimental purposes it is best to approximate this by

$$\frac{1}{q_n} \sum_{l=0}^{q_n - 1} \exp(2\pi i l\omega)(f^l(0) - R_\sigma^l(0))$$

as this avoids problems with windowing, since $q_n\sigma$ is almost an integer. All of our figures displaying spectra were calculated in this way.

The spectrum $\tilde{f}(\omega)$ should not be confused with the Fourier transform $\hat{\chi}_f(n)$ of $\chi_f(\theta) = h(\theta) - \theta$ where h is the conjugate homeomorphism of f; we now calculate their relationship. Using eq. (5.1) we know that $f^m(0) - R_\sigma^m(0) = \chi_f(m\sigma)$. Thus if $\omega = n\sigma \bmod 1$,

$$\begin{aligned}\tilde{f}(\omega) &= \lim_{L\to\infty} \frac{1}{L} \sum_{l=0}^{L-1} \exp(2\pi i n l\sigma)\chi_f(l\sigma) \\ &= \int_0^1 \exp(2\pi i n\theta)\chi_f(\theta)\, d\theta \quad \text{(by unique ergodicity)} \\ &= \hat{\chi}_f(n)\,. \qquad (6.2)\end{aligned}$$

(We will consistently denote Fourier series by ^.)

Thus the Fourier spectrum of χ just reorders the peaks of $\tilde{f}$ in increasing n. Let us consider in a little more detail how this occurs when $\sigma = \sigma_G$ so as to see why it is possible that, although $\hat{\chi}(n)$ is not universal as $n \to \infty$, $\tilde{f}(\omega)$ is universal as $\omega \to 0$. Let $\omega(n) = \inf\{|n\sigma - m| : m \in \mathbb{Z}\}$ denote the value of ω corresponding to n. Then using the relation (for $\sigma = \sigma_G$), $\omega(q_k) = |q_k\sigma_G - q_{k-1}|$ (with the q_k the Fibonacci numbers), we have that

$$\omega(n) = \sigma_G^k |r\sigma_G - s| ,$$

where $k = k(n)$, $r < s$ are positive integers such that k is the largest integer such that n can be written in the form $n = rq_k + sq_{k-1}$. In particular $\omega(n) \geqslant \sigma_G^{k+2}$, so we have that

$$\omega(n) \to 0 \Leftrightarrow k(n) \to \infty .$$

Since one will see that a large k is required for the corresponding peak to be universal, $\tilde{f}(\omega)$, $\omega \to 0$ is the object to study, and not $\hat{\chi}(n)$, $n \to \infty$.

The spectrum in fig. 12 has an envelope proportional to ω as $\omega \to 0$. For good winding numbers, this can be proven to be a strict upper bound by using the relationship (6.2) between $\tilde{f}$ and $\hat{\chi}$. We begin with a definition and a lemma which will be useful again in proving the scaling laws.

Definition. The *total variation* of a function F on an interval (a, b) is

$$\sup \sum_{i=1}^{N} |F(x_i) - F(x_{i-1})| , \tag{6.3}$$

where the supremum is taken over all N and over all choices $\{x_i\}$ such that $a = x_0 < x_1 < \cdots < x_N = b$.

If F is differentiable, then the total variation equals

$$\int_a^b |F'(x)| \, dx .$$

Lemma 6.2. Let F be a periodic function on [0, 1] of total variation B. Then $|\hat{F}(n)| \leqslant B/4n$.

Proof.

$$|\hat{F}(n)| = \left| \int_0^1 \exp(2\pi i n\theta) F(\theta) \, d\theta \right|$$

$$\leqslant \frac{1}{2} \int_0^1 \left| \exp(2\pi i n\theta) \left(F(\theta) - F\left(\theta - \frac{1}{2n}\right)\right)\right| d\theta$$

$$\leqslant \int_0^{1/2n} \sum_{i=1}^{2n} \left| F\left(\theta + \frac{i}{2n}\right) - F\left(\theta + \frac{i-1}{2n}\right)\right| d\theta$$

$$\leqslant \frac{B}{4n} . \qquad \text{Q.E.D.}$$

Now, since it is monotone, h has total variation one. Therefore, $\chi(\theta) = h(\theta) - \theta$ has total variation at most two, and thus $\hat{\chi}(n) \leqslant 1/2n$. If $\omega = n\rho - m$ and ρ is a good irrational then [8] for any $\epsilon > 0$ there is a $C_\epsilon > 0$ such that $n^{1+\epsilon} \geqslant C_\epsilon/\omega$. By eq. (6.2), $|\tilde{f}(\omega)| = |\hat{\chi}(n)| \leqslant 1/n \leqslant (\omega/C_\epsilon)^{1/(1+\epsilon)}$. For the golden mean C_0 can be set to σ_G^2, and therefore $|\tilde{f}(\omega)| < \sigma_G^{-2} \cdot \omega$.

Fig. 13 provides clear numerical evidence that the fractional corrections to the universal behavior of $\tilde{f}(\omega)$ are proportional to ω as $\omega \to 0$. In section 5 we conjectured (conjecture A) that any two cubic critical maps f, g with $\rho(f) = \rho(g) = \sigma \in A$ are related by a continuous change of coordinates $H_{f,g}$, continuously differentiable except for a first derivative discontinuity at $g(0)$. This implies that the difference in their spectra is

$$\tilde{f}(\omega) - \tilde{g}(\omega) = \lim_{L \to \infty} \frac{1}{L} \sum_{l=0}^{L-1} \times \exp(2\pi i l\omega)[H_{f,g}(g^l(0)) - g^l(0)]$$

$$= \lim_{L \to \infty} \frac{1}{L} \sum_{l=0}^{L-1} \exp(2\pi i l\omega) \chi_{f,g}(g^l(0)) , \tag{6.4}$$

where $\chi_{f,g}$ is periodic with period one and is

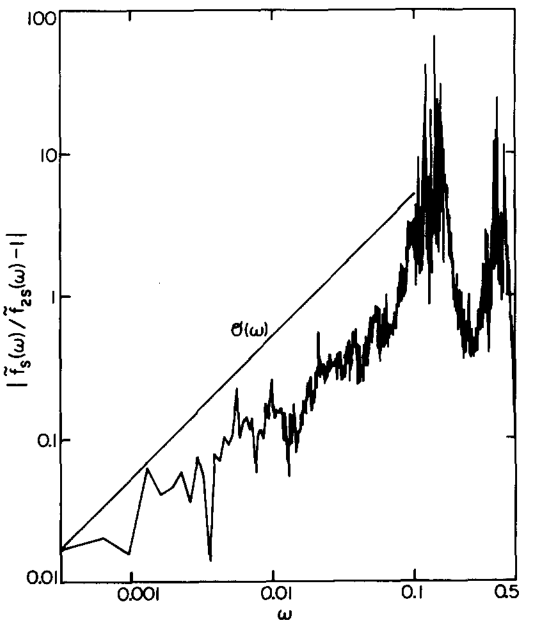

Fig. 13. Demonstration that the low frequency spectrum is universal with corrections that vary as ω. The comparison is between the two maps of fig. 7 with the same winding number as before. The same results were found for all other good irrationals that we studied.

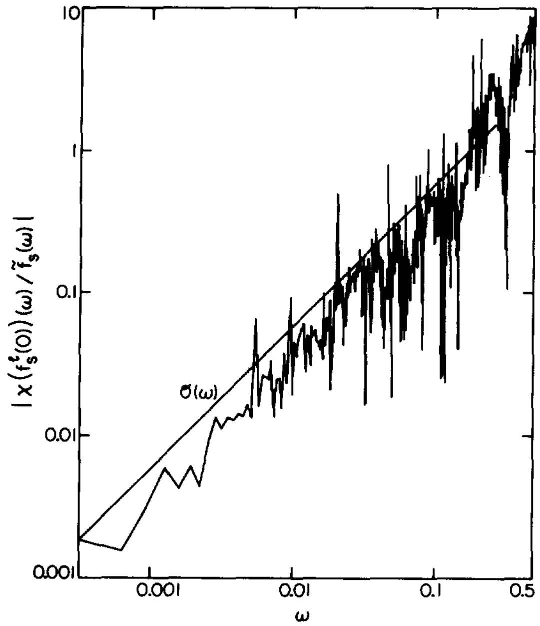

Fig. 14. Demonstration that the low frequency spectrum of a critical map is preserved by a smooth coordinate change. Following conjecture C we have plotted the normalised transform of the time series of a continuous periodic function, $\chi(x) = \sin(\pi x)$, $x \in [0, 1]$, composed with the sine map f_s for the winding number of fig. 7 (see eq. (6.5)).

differentiable except at $g(0)$ where it has a left and right derivative. Thus the following conjecture implies that

$$\tilde{f}(\omega) - \tilde{g}(\omega) = \mathcal{O}(\omega\tilde{g}(\omega)) \qquad (6.5)$$

and hence that as $\omega \to 0$ the structure of the spectrum is asymptotically independent of the mapping f, i.e. *$\tilde{f}$ is universal for small ω.*

Conjecture C. Let f be a cubic critical map with $\rho(f) = \sigma$ in A. Let P be periodic with period one and once differentiable except at $f(0)$ where it has left and right derivatives. Then as $\omega \to 0$,

$$\lim_{L\to\infty} \frac{1}{L} \sum_{l=0}^{L-1} \exp(2\pi i l\omega) P(f^l(0)) = \mathcal{O}(\omega\tilde{f}(\omega)) . \qquad (6.6)$$

We have not succeeded in proving this conjecture. Our evidence for its correctness is based on numerical experiments (see fig. 14 and caption). It may seem remarkably strong since the left-hand term in (6.6) equals $\widehat{P \circ h_f}(q_n)$ when $\omega = q_n\sigma \bmod 1$ and we believe that $\hat{\chi}_f(q_n) \sim 1/q_n$ whereas $\widehat{P \circ h_f}(q_n) \sim 1/q_n^2$. However, it is easy to see that there are many functions P for which (6.6) is true, e.g., $P(\theta) \equiv g^n(\theta) - \theta$. A simple calculation then makes plain why (6.6) only applies at small ω or equivalently that in $\widehat{P \circ h_f}(n)$ we consider only n for which $k(n) \gg 1$.

At this point we have a clear prescription. To analyze the experimental data, one must first extract the rotation number $\rho = \omega_1/\omega_2$ at the transition to chaos. If this rotation number is rational, the motion is phase-locked and periodic and no universality can be expected. One must tune the system away from these phase-locked states to an irrational rotation number. If $\rho = \sigma$ is irrational, compare the low frequency Fourier amplitudes of the time signal with those of the sine map (5.4) with

$a = 1$ and rotation number σ. Both spectra will have lots of structure, but the ratio should asymptote to a constant at low frequencies, with corrections that are uniformly bounded by a constant times ω.

For the rest of this section we shall again specialize to rotation numbers with periodic continued fractions, and in particular to the golden mean $\rho = \sigma_G$. Periodic continued fractions are of interest because of their characteristic self-similar spectra (fig. 11). The golden mean, among all rotation numbers, will presumably exhibit universality fastest in an experiment, since for a given length time series it allows the largest number of renormalisations.

Experiments performed with rotation number $\rho = \sigma_G$ will be least likely to phase lock, and hopefully will be easy to interpret.

In fig. 11, the main peaks at $\pm\sigma_G^j$ divide the spectrum into bands $B_j = \{\omega : \sigma_G^{j+2} < \omega < \sigma_G^{j+1}\}$. Despite the fact that the ω-axis in the figure is logarithmic, the peaks in any two bands are in a one to one correspondence. (Recall that all peaks are of the form $\omega = n\sigma_G - m$; thus if $\omega_i \in B_i$ then $\omega_{i+1} = -(n+m)\sigma_G + n = n\sigma_G^2 - m\sigma_G = \sigma_G\omega_i \in B_{i+1}$, and vice versa.) Band B_0 is of course cut in half (n.b., we assume $|\omega| < \frac{1}{2}$). Indeed, through this relationship the bands B_j partition the integers into "Fibonacci sequences", i.e., sequences Q_i where $Q_{i+1} = Q_i + Q_{i-1}$. The principal sequence ($Q_1 = 1$, $Q_2 = 1$) corresponds to the main peaks at $\omega = \sigma_G^i$. In order of decreasing amplitude, the next six peaks in a band correspond to the sequences with $(Q_1, Q_2) = (2, 2), (1, 3), (3, 3), (1, 4), (2, 5)$ *and* $(4, 4)$. The peaks corresponding to the sequence Q_1, Q_2, $Q_3 = Q_2 + Q_1, \ldots$ are positioned at $|r\sigma_G - s||\sigma_G|^i$ where $r = Q_1$ and $r + s = Q_2$.

Pictorially, it is clear in fig. 11 that $|\tilde{f}|$ scales as ω, and if we furthermore examine the phases, the apparent scaling law is

$$\tilde{f}(\omega) = -\sigma_G \tilde{f}(\omega/\sigma_G) + \mathcal{O}(\omega^2) \quad \text{as } \omega \to 0 . \tag{6.7}$$

We derive this law first for a piecewise linear fixed point of our renormalisation transformation. Then, using Conjecture C we shall deduce (6.7) for the physical strong-coupling fixed point f_*. Once proven for f_*, the scaling law then holds in general by conjectures B and C.

The conjugate homeomorphism h_* relating f_* to R_{σ_G} satisfies the following fixed point equations:

$$h_*(\theta) = \begin{cases} \alpha^{-1} h_*(-\theta/\sigma_G)\,, & -\sigma_G^2 < \theta \leqslant \sigma_G^3\,, \\ f_*^{-1}(\alpha^{-2} h_*((\theta/\sigma_G^2) - 1)\,, & \sigma_G^3 \leqslant \theta \leqslant \sigma_G\,. \end{cases} \tag{6.8}$$

The second equation involves the (nonlinear) function f_*^{-1} on $[\alpha^{-2}(\alpha-1)^{-1}, \alpha^{-1}(\alpha-1)^{-1}]$. From the fixed point equations for f_*, one can show that f_* sends $[\alpha^{-1}(1-\alpha)^{-1}, \alpha(\alpha-1)^{-1}]$ onto $[\alpha^{-2}/(\alpha-1), \alpha^{-1}/(\alpha-1)]$. We shall begin by replacing f_*^{-1} on this interval by the linear function

$$f_L^{-1}(\theta) = (\alpha^2 + \alpha)\theta + 1/(1-\alpha)\,,$$
$$\alpha^{-2}(\alpha-1)^{-1} < \theta < \alpha^{-1}(\alpha-1)^{-1}\,. \tag{6.9}$$

This function can be extended into a fixed point of the renormalisation transformation by interpolating linearly between its values at $\alpha^{-n}/(\alpha-1)$ (fig. 15):

$$f_L(\alpha^{-2n}/(\alpha-1)) = \alpha(\alpha-1)^{-1} - ((\alpha+1)/\alpha)^{n+1}\,,$$
$$f_L(\alpha^{-(2n+1)}/(\alpha-1)) = (\alpha-1)^{-1} - \alpha^{-1}((\alpha+1)/\alpha)^{n+1}\,. \tag{6.10}$$

A smooth curve drawn through the vertices (6.10) which define f behaves near zero as θ^x, where x satisfies

$$|\alpha|^{2x} - |\alpha|^{2x-1} - 1 = 0\,. \tag{6.11}$$

For a cubic inflection point ($x = 3$) $\alpha^6 + \alpha^5 - 1 = 0$ implies $\alpha = -1.2853$, quite close to the physical value -1.288575. (Note that f_L in (6.10) satisfies the fixed point equations for any $\alpha < 0$. When we compare f_L with f_* it will be for the correct value of α and therefore f_L will not scale exactly as θ^3 as

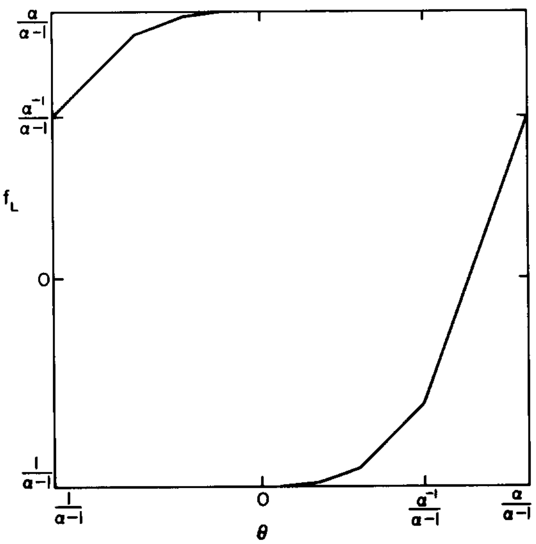

Fig. 15. A piecewise linear solution (6.10) of the fixed point equation for $\rho = \sigma_G$. The function plotted here behaves as θ^3 near the origin which fixes the value of α at -1.2853.

$\theta \to 0$.) Indeed, it also takes the correct value σ_G^{-1} at $x = 1$ (no singularity), and remains within $\approx 1\%$ of its (nonlinearized) physical value at least for $1 \leqslant x \leqslant 8$. We attach no great significance to this accuracy.

We now prove the scaling law for the linearized fixed point. If h_L conjugates f_L to R_σ then

$$h_L(\theta) = \begin{cases} \alpha^{-1} h_L(-\theta/\sigma_G), & -\sigma_G^2 < \theta < \sigma_G^3, \\ (1+\alpha^{-1}) h_L((\theta/\sigma_G^2) - 1) + 1/(1-\alpha), & \sigma_G^3 \leqslant \theta \leqslant \sigma_G. \end{cases} \tag{6.12}$$

For computational ease let $\chi_L(\theta) = h_L(\theta) - \theta + \sigma_G + \alpha/(1-\alpha)$. (The added constant insures $\chi_L(-\sigma_G^2) = \chi_L(\sigma_G) = 0$ and changes only the constant term in the Fourier expansion.) Then define $\chi_L \equiv \chi_h + \chi_i$ where

$$\chi_i(\theta) = \begin{cases} -(\theta + \sigma_G^2)(\sigma_G + \alpha^{-1})/\sigma_G, & -\sigma_G^2 < \theta < \sigma_G^3, \\ (\theta - \sigma_G)(\sigma_G + \alpha^{-1})/\sigma_G^2, & \sigma_G^3 \leqslant \theta \leqslant \sigma_G, \end{cases} \tag{6.13}$$

Then χ_i is continuous and its Fourier transform $\hat{\chi}_i(n) \sim 1/n^2$. The function χ_h then satisfies

$$\chi_h(\theta) = \begin{cases} \alpha^{-1}\chi_L(-\theta/\sigma_G), & -\sigma_G^2 \leqslant \theta \leqslant \sigma_G^3, \\ (1+\alpha^{-1})\chi_L(\theta/\sigma_G^2 - 1), & \sigma_G^3 \leqslant \theta \leqslant \sigma_G. \end{cases} \tag{6.14}$$

Let $\omega = |q_j\sigma_G - q_{j-1}|$, where $\{q_n\}$ for the remainder of this section is any integer series satisfying $q_{n+1} = q_n + q_{n-1}$, i.e., a Fibonacci sequence. Then $\omega \gtrsim 1/q_j$, so terms $\mathcal{O}(1/q_j)$ are $\mathcal{O}(\omega)$. Then letting $\sigma = \sigma_G$,

$$\tilde{f}_L(\omega) = \hat{\chi}_L(q_j) = \hat{\chi}_h(q_j) + \mathcal{O}(\omega^2), \tag{6.15}$$

$$\begin{aligned} \hat{\chi}_h(q_j) &= \int_{-\sigma^2}^{\sigma} \exp(2\pi i q_j\theta)\chi_n(\theta)\,d\theta \\ &= \alpha^{-1}\sigma \int_{-\sigma^2}^{\sigma} \exp(-2\pi i q_j\sigma\theta)\chi_L(\theta)\,d\theta \\ &\quad + (1+\alpha^{-1})\sigma^2 \\ &\quad \times \int_{-\sigma^2}^{\sigma} \exp(2\pi i q_j(\theta+1)\sigma^2)\chi_L(\theta)\,d\theta \\ &= \alpha^{-1}\sigma\hat{\chi}_L(-q_{j-1}) + (1+\alpha^{-1})\sigma^2\chi_L(q_{j-2}) \\ &\quad + \alpha^{-1}\sigma\omega \int_{-\sigma^2}^{\sigma} \exp(-2\pi i q_{j-1}\theta) \\ &\quad \times \left(\frac{\exp(-2\pi i\omega\theta) - 1}{\omega}\right)\chi_L(\theta)\,d\theta \\ &\quad + (1+\alpha^{-1})\sigma^3\omega \int_{-\sigma^2}^{\sigma} \exp(2\pi i q_{j-2}\theta) \\ &\quad \times \left(\frac{\exp(2\pi i\omega\sigma(\theta+1)) - 1}{\omega\sigma}\right)\chi_L(\theta)\,d\theta\,. \end{aligned} \tag{6.16}$$

The last two integrals are ω times Fourier transforms of functions of bounded variation; by lemma 6.1 these terms are $\omega\mathcal{O}(1/q_n)$ and thus $\mathcal{O}(\omega^2)$. Using relation (6.2) again, we have finally

$$\tilde{f}_L(\omega) = \alpha^{-1}\sigma_G \tilde{f}_L(\omega/\sigma_G) + (1+\alpha^{-1})\sigma_G^2 \tilde{f}_L(\omega/\sigma_G^2) + \mathcal{O}(\omega^2)\,, \tag{6.17}$$

The eigenvalues of this second order linear recursion relation which relates $\tilde{f}_L(\omega)$ to $\tilde{f}_L(\omega/\sigma_G)$ are $-\sigma_G$ and $\sigma_G(1+\alpha^{-1}) \approx -0.288\sigma_G$. The first dominates, and its eigenspace gives the scaling law (6.7). Note that (6.7) implies $|\tilde{f}(\omega)| \approx \omega$ and gives a sign change between successive bands B_j in fig. 11.

To show scaling for the cubic strong-coupling fixed point f_*, one must include a correction in the fixed point equations (6.12), which accounts for the nonlinearity of f_*^{-1} on $(\alpha^{-2}/(\alpha-1),\ \alpha^{-1}/(\alpha-1))$. Let

$$\begin{aligned} &f_*^{-1}(\theta) = f_L^{-1}(\theta) + X(\alpha^2\theta)\,,\\ &\alpha^2/(\alpha-1) \leqslant \theta \leqslant \alpha^{-1}/(\alpha-1)\,, \end{aligned} \tag{6.18}$$

where X is periodic with period one and analytic except at $\alpha/(\alpha-1)$. The analysis proceeds as before, with an additional term. Let $\chi^* = \chi_h^* + \chi_i$, $(\chi^*(\theta) \equiv h_*(\theta) - \theta + \sigma_G - \alpha/(\alpha-1)$ as before); then using σ to denote σ_G,

$$\begin{aligned} \hat{\chi}^*(q_j) + \mathcal{O}(\omega^2) &= \chi_h^*(q_j)\\ &= \alpha^{-1}\sigma\hat{\chi}^*(-q_{j-1}) + (1+\alpha^{-1})\sigma^2\hat{\chi}^*(q_{j-2})\\ &\quad + \alpha^{-1}\sigma\omega \int_{-\sigma^2}^{\sigma} \exp(-2\pi i q_{j-1}\theta)\\ &\quad \times \left(\frac{\exp(2\pi i\omega\theta)-1}{\omega}\right)\chi^*(\theta)\,d\theta\\ &\quad + \sigma^3\omega \int_{-\sigma^2}^{\sigma} \exp(2\pi i q_{j-2}\theta)\\ &\quad \times \left(\frac{\exp(2\pi i\omega\sigma(\theta+1))-1}{\omega\sigma}\right)\\ &\quad \times ((1+\alpha^{-1})\chi^*(\theta) + \chi(h_*(\theta)))\\ &\quad + \sigma^2 \int_{-\sigma^2}^{\sigma} \exp(2\pi i q_{j-2}\theta) X(h_*(\theta))\,d\theta\,. \end{aligned} \tag{6.19}$$

The first two integrals as before are $\mathcal{O}(\omega^2)$ by lemma 6.2. The last integral satisfies the conditions of conjecture C; it is thus $\mathcal{O}(\omega\hat{\chi}^*(q_j))$ which by lemma 6.2 must be $\mathcal{O}(\omega^2)$ and (6.17) holds for f_*. Thus if $\chi_n(q_j) \sim (1/q_j)^\nu$ then $\nu = 1$ and therefore the linearised fixed point equations determine the scaling laws but not the coefficients.

Thus as in the period doubling cascade, the universal features of the onset of chaos are associated with small fluctuations on very long time scales. Here, however, no new frequency peaks appear. Rather, it is the increasing importance of low frequency resonances of the principal frequencies that heralds the transition. Based upon reasonable conjectures, we have been able to show that for good winding numbers these low frequency resonances at the transition are universal, and that they scale and are self-similar for winding numbers with periodic continued fractions.

7. Ergodic renormalisation for random continued fractions

Most of the above analysis has been for rotation numbers $\sigma = [n_1, n_2, \ldots]$ with a periodic continued fraction. Although conjectures A–C apply to any good irrational and were checked numerically for non-periodic continued fractions (cf., figs. 7, 12–14), we have done several numerical experiments iterating the renormalisation transformations for a small number of cubic critical maps where the entries n_i in the continued fraction of the rotation number is a random sequence of bounded integers. The results of these lead us to make the following conjecture.

Conjecture D. Let f and g be cubic critical maps with $\rho(f) = \rho(g) = \sigma = [n_1, n_2, \ldots] \in A$. Then

$$[T_{n_j} \circ \cdots \circ T_{n_2} \circ T_{n_1}(f)] - [T_{n_j} \circ \cdots \circ T_{n_2} \circ T_{n_1}(g)] \tag{7.1}$$

converges to zero as $j \to \infty$.

There is clearly an intimate connection between (7.1) and the low frequency universality of the spectra (fig. 14). For example, we find numerically that if f is given by (5.4) and $g(x) = x^3 + \omega$, (2.11) and

$$\sigma = [2, 2, 1, 1, 2, 1, 1, 2, 1, 1, 1, 1, 2, 2, 2, 2, 2, \ldots],$$

then for $j = 0$, (7.1) is 0.02515 ... (in the sup norm) while if $j = 9$, (7.1) is 0.00020.... Using our numerical methods it is not reasonable to estimate (7.1) for higher values of j because of the limitations of the machine accuracy in controlling the rotation number.

We believe one should look at this sutiation as follows. Let $g : [0, 1] \to [0, 1]$ be defined by

$$g(\lambda) = \lambda^{-1} - [\lambda^{-1}],$$

where $[\beta]$ is the integer part of β. Then g preserves a unique probability measure (whose support is a set of full measure) $\mu = G(x)\,\mathrm{d}x$ on [0, 1] where

$$G(x) = (\log 2)^{-1}(1 + x)^{-1}$$

and this measure is ergodic [23]. Let B denote the set of all those λ in Herman's set A whose trajectory under g is distributed on [0, 1] with density $G(x)$. By the ergodic theorem, this is a set of Lebesgue measure 1. Define a mapping $\tilde{T}_R$ as follows

$$\tilde{T}_R(f) = \tilde{T}_{[\rho(f)^{-1}]}(f).$$

This mapping leaves invariant the set of those critical maps f with $\rho(f) \in B$. Our conjecture is this:

Conjecture E. There is an uncountable set Λ of generic critical maps which is invariant under T_R and has the following properties:

(i) if $f \in \Lambda$ then $\rho(f) \in B$,
(ii) if $\rho(f) \in B$ then $T_R^n(f) \to \Lambda$ as $n \to \infty$,
(iii) the action of T_R on Λ is ergodic, and
(iv) the Liapunov exponents [24] $\chi_1 \geqslant \chi_2 \geqslant \cdots$ of T_R are such that $\chi_1 > 0 > \chi_2$.

The idea is that χ_1 corresponds to $\log|\delta|$; all other exponents correspond to contraction towards Λ. Thus if the conjecture is correct we have an example of an ergodic renormalisation attractor with a highly non-trivial structure of stable and unstable manifolds [24]. Also, we have the universal numbers $\chi_1, \chi_2, \ldots$ which are essentially independent of rotation number. However, it is not clear whether or not their physical interpretation is of any real use.

A clearer picture emerges if instead of critical maps we work with diffeomorphisms. Then the maps $T_1, T_2, \ldots$ preserve the one-dimensional subspace $\{R_\lambda : 0 \leqslant \lambda < 1\}$ consisting of pure rotations. Thus T_R maps the space $\{R_\lambda : \lambda \in B\}$ to itself. Identifying this space with B, it is clear that the restriction of T_R to it is just $g(\lambda) = \lambda^{-1} - [\lambda^{-1}]$. Thus the derivative of T_R at $\lambda \in B$ is $-\lambda^{-2}$ and we can calculate the expanding Liapunov exponent in the direction of this subspace. It is

$$\chi_1 = \int_0^1 \log(\lambda^{-2}) G(\lambda)\,\mathrm{d}\lambda = \pi^2/(6 \log 2).$$

We conjecture that all other exponents are negative and that B is the ergodic attractor of T_R on diffeomorphisms.

8. Invariant circles in higher dimensions

We now indicate how we believe the above theory applies to diffeomorphisms of the multidimensional annulus $\mathbb{R}^n \times \mathrm{T}^1$ and hence to differential equations. The discussion follows the treatment of Collet, Eckmann and Koch [25] for the Feigenbaum transformation. For clarity, we only discuss the 2-dimensional case ($n = 1$), but it should be clear that our arguments are equally valid in the higher dimensional situation. We also restrict here to the case $\sigma = \sigma_G$.

Our main concern is with diffeomorphisms of the annulus which possess a single invariant circle with rotation number σ. In fact, as in the

1-dimensional case, it is necessary to work with a larger class of mapping which are defined in the following fashion. Let $\mathscr{B}$ denote the space of all pairs (E, F) of orientation-preserving maps of the plane $\mathbb{R}^2$ to itself. The annulus maps are embedded in $\mathscr{B}$ exactly as circle maps are embedded in $\mathscr{S}$. Let

$$E_*(r, \phi) = (0, \xi_*(\sqrt[3]{\phi^3 + r})),$$
$$F_*(r, \phi) = (0, \eta_*(\sqrt[3]{\phi^3 + r})), \tag{8.1}$$

where (ξ_*, η_*) is the strong-coupling fixed point of $T = T_1$. If, as we claim, (ξ_*, η_*) exists, then by lemma 3.2 it is an analytic function of x^3 and therefore E_* and F_* are analytic functions of (r, ϕ).

Let $\Lambda(r, \phi) = (\alpha^3 r, \alpha\phi)$ where $\alpha = (\eta_*(0) + 1)/\eta_*(0)$. Now let $\mathscr{B}_0$ be a small neighbourhood of (E_*, F_*) in $\mathscr{B}$ chosen so that the mapping $\mathscr{T}: \mathscr{B}_0 \to \mathscr{B}$ given by

$$\mathscr{T}(E, F) = (\Lambda F \Lambda^{-1}, \Lambda F E \Lambda^{-1}) \tag{8.2}$$

is well defined. Clearly, (E_*, F_*) is a fixed point of $\mathscr{T}$.

Moreover (E_*, F_*) defines a (singular) map of the annulus in the way defined by the following construction. Suppose that E and F have the following special properties: a) there are four curves γ_0, $\gamma_1^\pm$, and γ_2 of the form $\phi = u_0(r)$, $\phi = u_1^\pm(r)$ and $\phi = u_2(r)$ where $u_1^-(r) < u_0(r) < u_2(r) < u_1^+(r)$ and $(0,0) \in \gamma_0$ such that $E(\gamma_1^-) = \gamma_2$, $E(\gamma_0) = \gamma_1^+$ and $F(\gamma_1^+) = \gamma_2$; b) E maps the region R_1 between γ_1^- and γ_0 into the region R_2 contained between γ_0 and γ_1^+ and F maps R_2 into $R = R_1 \cup R_2$ (fig. 16); c) if the mapping

$$P = P(E, F): R \to R$$

is such that $P = E$ on R_1 and $P = F$ on R_2 (so that P is 2-valued on γ_0), then R contains a P-invariant curve of the form $r = v(\phi)$ for some continuous v with $v(0) = 0$, and for all x in R, $P^n(x) \to \Gamma_P$ as $n \to \infty$. Then glueing P along γ_1^- and γ_1^+ we get a piecewise-analytic map of the annulus. To see how $\mathscr{T}$ acts on P see fig. 17.

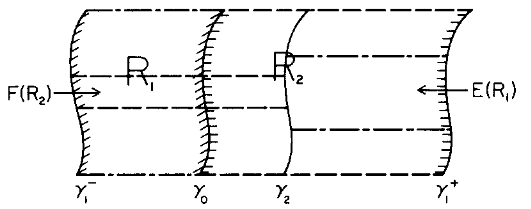

Fig. 16. Schematic representation of the construction of an annular mapping from a pair (E, F) of homeomorphisms of $\mathbb{R}^2$.

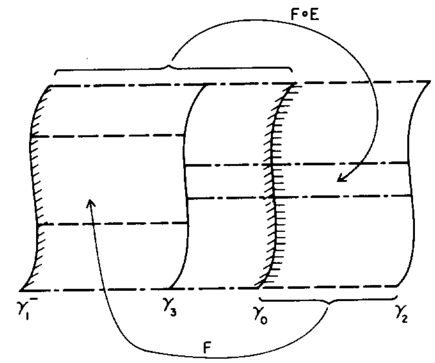

Fig. 17. Schematic representation of how $\mathscr{T}$ acts upon $P = P(E, F)$.

If $P_* = P(E_*, F_*)$ then $r = 0$ is an invariant curve for P_*; the restriction of P_* to $r = 0$ is just the 1-dimension strong-coupling fixed point and the curves $r + \phi^3 = \text{const.}$ are mapped to a single point on $r = 0$ in one iteration of P.

(The form of (8.1) can now be made plausible by anticipating several constructions contained in the appendix. Below the transition, the strong stable foliation of v intersects v transversely whereas at the transition it is tangent.

Iteration of the map wraps the tangent point around the invariant curve and increases the contraction while applying T then retains only one tangent point. The tangency must be cubic by construction and at the fixed point the contraction rate is effectively infinite; the entire curve $r + \phi^3 = \text{const.}$ is collapsed in one iteration of the map to a point.)

Returning now to the full neighbourhood $\mathscr{B}_0$ of (E_*, F_*), our conjecture is as follows: *the eigenvalues λ of the linearisation* $\mathrm{d}\mathscr{T}(E_*, F_*)$ of $\mathscr{T}$ at (E_*, F_*) with $|\lambda| \geqslant 1$ are ± 1, $\pm\alpha$, α^2, $\pm\alpha^3$, δ, where α and δ are calculated from (ξ_*, η_*). Of these we can eliminate all but the eigenvalues α^2 and δ which have multiplicity one in the following way:

a) the eigenvectors corresponding to $+1$, α and α^3 are the infinitessimal generators of coordinate transformations and therefore are irrelevant and can be removed as in [25], b) the eigenvectors corresponding to -1, $-\alpha$ and $-\alpha^3$ are not tangent to the space $EF = FE$. The eigenvector corresponding to δ (resp. α^2) is $((0, X(\sqrt[3]{\phi^3 + r}), (0, Y(\sqrt[3]{\phi^3 + r}))$ where (X, Y) is the eigenvector corresponding to δ (resp. α^2) for $\mathrm{d}T(\xi_*, \eta_*)$.

Factoring out the coordinate changes as in [25] and restricting to the space of commuting functions $EF = FE$, we have the following picture. The fixed point (E_*, F_*) of $\mathscr{T}$ has a 2-dimensional unstable manifold and a co-dimension 2 stable manifold W^s. Any two-parameter family of annulus mappings which is transverse to W^s will have the scaling behaviour associated with the 1-dimensional generic critical maps. In particular the values of α and δ obtained by approximation by p_n/q_n-cycles will be the same as in 1 dimension, as has been numerically verified by Shenker [11]. The way an invariant circle with rotation number σ breaks up is independent of the family.

A similar analysis can be given for non-critical maps and the weak-coupling fixed point. In that case we take the scaling matrix to be $\Lambda = -\sigma I$.

9. Conclusion

Let us review as clearly as possible how one might perform an experiment to explore the transition to chaos proposed here. Two experimental parameters must be consistently varied. The Rayleigh number R is clearly one parameter, while the second should permit direct control of the frequency ratio in the quasi-periodic regime. An obvious choice is to periodically modulate (frequency ω_2), a periodic regime of flow (frequency ω_1). A periodic external force has the added advantage of making a Poincaré section trivial to compute. (In particular the Fourier transform of the distribution of points on the section should be measurable with an accuracy comparable to the power spectrum.)

The transition should be approached for a fixed irrational value of ω_1/ω_2 by increasing R. Although any "good" irrational will do, the optimal choice experimentally is $\omega_1/\omega_2 = \sigma_G = (\sqrt{5} - 1)/2$. The golden ratio is the least susceptible to mode locking, which is to be avoided, and for a given level of resolution allows the quickest approach to the universal limit. Alternatively put, σ_G gives the largest number of self-similar bands for a given level of noise.

It would clearly be of interest to do such an experiment for a finite dimensional system such as a van der Pol oscillator. Just as for period doubling universality means certain features of the power spectra will be system independent.

Only the low frequencies $\omega \ll \omega_1, \omega_2$ are universal so data should be collected for as long as possible but in any event for a time which is a Fibonacci multiple of $2\pi/\omega_2$. The quasi-periodic signal will then effectively repeat; facilitating the Fourier transform. To within an overall complex factor, all the low frequency Fourier amplitudes at a transition should agree in magnitude and phase as $\omega \to 0$ with the values obtained from a map such as (2.7).

Although the renormalisation group and fixed point calculations are highly discontinuous with winding number, all our predictions are completely continuous in so far as experiment is concerned. Small errors in the frequency ratio are only apparent as $\omega \to 0$. Spectra will approach a universal form as $\omega \to 0$ and only deviate for ω on the scale of the error. Similar comments apply to the control of R. Just below the transition at R_c the power in the principal peaks at $\omega = \sigma_G^n$ will scale as ω^2 down to $\omega \approx \mathrm{const.}|R - R_c|^{|\ln(\sigma_G)|/(2\ln|\alpha|)}$ and then fall off rapidly as $\exp(-\mathrm{const.}/\omega)$. Above the transition there will be a slight broadening of all peaks with the very lowest frequencies indistinguishable from the noise.

More elaborate tests of the universal theory, such as a direct measurement of δ, can be devised by examining the spectra in the various mode locked states that approximate σ_G. We still expect the simplest and most precise experiment to be the one above.

The Couette system would appear to be a favorable geometry in which to test our predictions since it does not mode lock [26]. Control over the frequency ratio could be achieved by working in the wavy vortex regime and modulating the rotation speed. However, the rotational invariance that eliminates the mode locking makes it implausible to us that at the transition Couette flow can be described by our universality class. It is therefore doubtful whether one will observe our universal spectrum. We have no hard demonstration of these assertions, but it is obvious that if the parameters in any non-trivial one-dimensional map are varied without constraint within an open set, mode locking will result.

It is still of interest to examine the low frequency spectrum for a rotationally invariant system at the transition. Model studies indicate that even if $\omega_1/\omega_2 = \sigma_G$, a singular power spectrum whose envelope is bounded by some power of ω might be seen that nevertheless is not self-similar in the sense of fig. 11. It is also possible that the weight in the low frequency peaks will fall exponentially at the transition. In this case it is very doubtful whether there are any quantitatively universal features at the transition.

The transition to chaos we have examined which entails the destruction of an invariant torus in the presence of strong radial contraction is different from the example analysed by Ruelle, Takens and Newhouse [27]. They examined, in the weak coupling limit, flow on an $n \geqslant 3$ torus and showed for any preassigned degree of smoothness a small perturbation could be added to the original quasiperiodic flow with n frequencies to render it chaotic. Of course this chaos would only be visible at very long times.

Flow on an n-torus could also mode lock to produce a 2-torus; and one might ask whether such a 2-torus in the strong coupling limit could break down chaotically to a flow that remains on the $n > 2$ torus. We are uncertain whether all models of this sort must fall into our universality class. We have specific examples where the transition is continuous and the rotation number periodic (e.g., σ_G) which exhibit qualitatively different spectra. We have also seen in a mapping in which one of the variables was constrained to be a simple rotation a continuous transition to chaos characterized by singular power spectra where the position of the prominent lines shows no simple relation to the rotation number. A simple explanation of these findings in the present context is in terms of chaotic renormalization group trajectories. This conjecture differs in detail from section 7 since the rotation number now is fixed and periodic. The relevance of this model to any physical system remains to be established.

Mathematically, our paper consists of a number of conjectures. The simplest is the existence of the strong-coupling fixed point. Presumably, a rigorous proof of this along the lines of Lanford's computer-assisted proof of the Feigenbaum conjectures should be possible [18]. But more interesting are the conjectures A, B and C (and the numerical evidence supporting them) where we conjecture the existence of C^1 conjugacies between certain critical maps. We have no idea of how to prove these and it is clear that the techniques developed for diffeomorphisms as in [7] are of little use here. Finally, we remark that it would be interesting to have a proof of the ergodic renormalisation structure conjectured in section 7. New ideas will be needed for the proof of this.

Anyone who has examined the other small divisor problems to which K.A.M. methods have been applied would not have failed to notice the obvious similarities in proof. It is natural to ask to what extent these problems admit a strong coupling limit where the K.A.M. properties (e.g., analytic conjugacies, etc.) disappear continuously through a loss of smoothness.

The first problems to be investigated from this viewpoint were Hamiltonian systems, in particular area preserving maps, in action-angle variables (r, ϕ) [14, 28, 29]. The spectra of the homeomorphism that conjugates the phase variable along a particular critical K.A.M. surface to a pure rotation closely resembles the one computed here for cubic critical maps. There is a natural way to generate a critical circle map in the area preserving problem by simply restricting the 2-D map to the invariant K.A.M. curve. For the golden mean this map is found numerically to be C^1 and have no critical points.

Since the map is clearly critical by virtue of its singular invariant measure it is natural to ask whether under T it would be attracted to any of the fixed points associated with inflectional circle maps, possibly non-analytic ones, e.g., (2.11). The answer is probably no, on empirical grounds.

We varied the inflectional exponent b in (2.11) so as to obtain the same value of α as in ref. 29. We found $b = 1.82047$ gave $\alpha = 1.41485$. The spectra however did not agree. Whether anything can be said about the Hamiltonian problem from knowledge of the dissipative case remains to be seen.

It is worth noting that the fixed point we have found in dissipative systems is much more robust than can possibly be true for conservative systems. Whereas universality has been demonstrated for one degree of freedom area-preserving maps [28, 29], a continuum system will possess an infinity of frequencies. It is only through imposition of external fields or boundary conditions that a few degrees of freedom can be singled out. We know from laboratory experiment and rigorous mathematics that continuum dissipative systems can have low dimensional attractors (e.g., 2-tori).

The spectrum of quasi-periodic Hermitian operators (e.g., the Schrödinger equation with a quasi-periodic potential) is another small divisor problem of current interest [30]. Self-similarity in the distribution of band gaps as a function of winding number for a particular "critical" potential was noted by Hofstadter [31]. The problem of searching for extended states is equivalent to constructing a $(n + 1)$-torus in a nonlinear system for which in certain cases n of the phases evolve according to a free rotation with mutually incommensurate frequencies. When $n = 2$ our renormalization group may be used to evaluate the string of matrix products (which each depend on a phase, ϕ, on which T acts), whose trace determines the Liapunov exponent of a particular state. One then generates a renormalisation transformation on the matrices (e.g., when ϕ_i lies in the interval removed by T multiply $M(\phi_i)$ with its predecessor ϕ_{i-1} and call it $M^2(\phi_{i-1})$).

After i applications one reduces the original matrix string to products of M^{q_i}, $M^{q_{i-1}}$. This grouping of the matrix multiplications is identical to the decimation scheme introduced in a different context by Feigenbaum and Hasslacher [32].

Finally we note that Manton and Nauenberg [33] have observed self-similar and singular behaviour at the limiting radius of convergence for the Schröder problem.

Acknowledgments

The authors would like to thank M. Feigenbaum, L.P. Kadanoff and Scott Shenker for communicating their results prior to publication and for conversations. J. Guckenheimer, P.C. Hohenberg, R. McKay and L. Jonker also made a number of valuable suggestions. We were supported in part by a Sloan Foundation Grant (E.D.S.) and by a National Science Foundation Grant, number PHY77-27084. Considerable credit for this work goes to the Institute for Theoretical Physics which brought the four of us together.

Appendix A

Transition from quasi-periodicity via phase-locking

We discuss here some details concerning the ways in which phase-locked invariant tori can be destroyed and then relate this to the case studied above. Firstly, we consider a prototypical example involving the creation of a *critical cycle*. Then using the computer study of Aronson, Chory, Hall and McGehee [34] we give a heuristic discussion of the bifurcation structure within a single phase-locked region. Much of this structure can be related to (not necessarily invertible) maps of the circle onto itself. After discussing this, we attempt to relate this picture to the case where the system is not phase-locked, as studied above.

Consider a two-parameter family $P_{\omega,a}$ of diffeomorphisms of the annulus A into itself which contracts areas uniformly and where the nonlinear coupling a and the rotation ω enter as in the family (1.1) discussed in the introduction, i.e., as the relevant parameters of our renormalisation group. We first consider the bifurcations observed when a is small. To do this we need to consider the structure of the *saddle-node bifurcation* in a little more detail.

Consider a one-parameter family P_μ of such mappings (e.g., $P_\mu = P_{\omega(\mu),a(\mu)}$). The conditions for a fixed point x of P_μ to undergo a saddle-node bifurcation at $\mu = 0$ are the following: (a) the derivative $\mathrm{d}P_0(x_0)$ of P_0 at x_0 has 1 as a simple eigenvalue and no other eigenvalues of modulus equal to 1; (b) for $|\mu|$ small there are coordinates $(s, z, \mu) \in \mathbb{R} \times \mathbb{R} \times (-1, 1)$ on a neighbourhood of $(x_0, 0)$ in $A \times (-1, 1)$ such that $(x_0, 0)$ is the origin and in this neighbourhood

$$P_\mu(x, z) = (g_\mu(s), k_\mu(z)),$$

where $g_0(0) = 0$, $g_0'(0) = 1$, $g_0''(0) \neq 0$, $\partial g_\mu(0)/\partial\mu|_{\mu=0} \neq 0$ and $|\mathrm{d}k_0(0)| < 1$. Then the family g_μ can be conjugated with the family $\tilde{g}_\mu : \mathbb{R} \to \mathbb{R}$ given by $\tilde{g}_\mu(s) = s + s^2 + \mu$. Thus the mapping $(s, z, \mu) \to (s + s^2 + \mu, z/2, \mu)$ is a universal *local* model for the saddle-node.

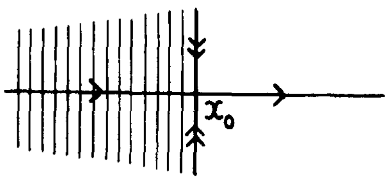

Fig. 18. The local structure of a saddle node. The "vertical" lines represent the strong-stable foliation.

At $\mu = 0$, locally near x_0 the situation is as shown in fig. 18. Near x_0, the *outset* $\{x : P_0^{-n}x \to x_0$ as $n \to \infty\}$ consists locally of the curve $\{z = 0, s \geqslant 0\}$; near x_0, the *inset* $\{x : P_0^n x \to x_0$ as $n \to \infty\}$ consists of the half-space $\{s \leqslant 0\}$. Moreover, there is a *strong stable foliation* of the local inset defined as follows: it is the partition of the inset into curves (called *strong stable leaves*) defined by the following rule: x and y lie in the same leaf if and only if $\mathrm{dist}(P_0^n x, P_0^n y)$ converges to zero exponentially fast as $n \to \infty$. This foliation is invariant under P_0 in the sense that the P_0-image of a leaf is contained in a leaf. Moreover, along $z = 0$, the tangents to these leaves depend continuously upon the base point. In some neighbourhood of x_0 the leaves are all transverse to the centre manifold $z = 0$. For a proof of all these facts see Newhouse, Palis and Takens [35]. The saddle-node bifurcation for periodic orbits is covered by the above description (if the period is q, replace P by P^q).

We now consider the sequence of bifurcations involved in phase-locking when a is small and the invariant circle is preserved (see fig. 19). (Again, without loss of generality we can restrict to the case of a fixed point.) The bifurcations at $\mu = \mu_0$ and μ_1 are saddle nodes. We shall only consider the bifurcation at $\mu = \mu_1$. Assume $\mu_1 = 0$. Here the invariant circle is the outset of the saddle-node. Since the outset is contained in the inset we have a *cycle* and this will force the bifurcation to have a non-trivial global structure even though the local structure (at the fixed point) is simple.

Assume that the outset $\mathcal{O}$ is transverse to each strong stable leaf. Then using invariant manifold theory (Hirsch, Pugh and Shub [3]) one can prove that $\mathcal{O}$ is smooth and normally hyperbolic. Therefore for small $\mu \geqslant 0$ there are smooth invariant circles $\mathcal{O}_\mu$ near $\mathcal{O} = \mathcal{O}_0$ which depend smoothly upon μ.

At $\mu = 0$, P_0 has a fixed point (on $\mathcal{O}_0$). For small $\mu > 0$, P_μ has no fixed point. Therefore for all $\epsilon > 0$ there exists a set K in $(0, \epsilon)$ of positive Lebesgue measure such that if $\mu \in K$ then the rotation number is irrational (Herman [8]). One expects that generically the closure of K is a Cantor set. If $\mu \in K$ the

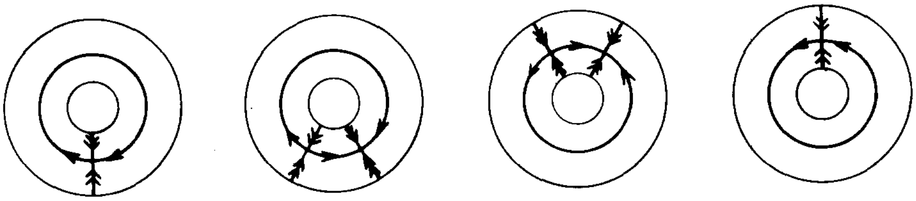

Fig. 19. The bifurcations creating and destroying a phase-locked (periodic) attractor on the invariant circle while staying within the quasi-periodic regime (i.e., preserving the invariant circle).

attractor is the whole circle $\mathcal{O}_\mu$. Thus we see that even in this controlled situation there is an *explosion* from a point attractor to a circle attractor. Nevertheless, for $\mu > 0$, the behaviour is still quasi-periodic. Thus we see that to destroy the quasi-periodicity we must not have transversality of $\mathcal{O}$ to the strong stable foliation.

Consider again the sequence of bifurcations shown in fig. 19 above. We discuss the simplest change to this which produces a bifurcation away from quasi-periodicity. This is achieved if at some intermediate value of μ, say $\mu = \mu_2$, $\mu_0 < \mu_2 < \mu_1$, the invariant circle loses its smoothness by becoming tangent to the (local) strong stable foliation defined near the sink so that for $\mu_2 < \mu < \mu_1$ the circle has quadratic tangencies with some of the leaves of this foliation. (The foliation is defined as follows. Assume that the eigenvalues of the sink are such that $0 < \lambda_1 < \lambda_2 < 1$. Then define the leaves by the condition that two points x and y lie in the same leaf if dist($P^n x$, $P^n y$) dist($P^n x$, $P^n y$) $\approx \lambda_1^n$.) The leaf through the sink is called the *strong stable manifold.*

Then the important point to note is that at $\mu = \mu_1 = 0$, $\mathcal{O}$ is tangent to the strong stable foliation of the saddle-node and the tangencies are quadratic (fig. 20). Then (a) for small $\mu > 0$ there is no invariant circle, (b) for all $\epsilon > 0$ there is a μ in $(0, \epsilon)$ such that P_μ has a horseshoe, and (c) there exists a sequence $\mu_i > 0$ such that $\lim_{i\to\infty} \mu_i = 0$ and P_{μ_i} has a homoclinic tangency for each i [35].

Thus one sees that here the dynamical behaviour

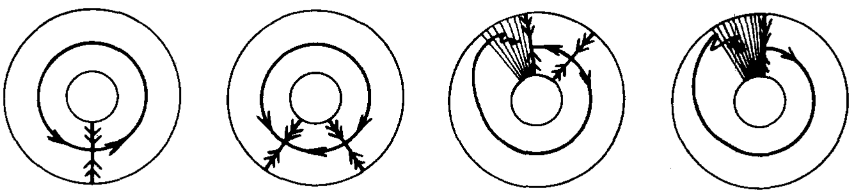

Fig. 20. The simplest sequence of bifurcations creating and destroying the phase-locking and destroying the invariant circle. At $\mu = \mu_0$ there is a generic saddle-node creating the (phase-locked) periodic solution. At $\mu = \mu_2$ the outset of the saddle becomes (cubically) tangent to the strong stable foliation of the sink. For $\mu_2 < \mu < \mu_1$, the outset is quadratically tangent to this foliation. At $\mu = \mu_2$ the outset is quadratically tangent to the foliation defined by the saddle node point.

for $\mu > 0$ is very different from that in the previous bifurcation. In that case there was always an essentially global attractor which was periodic or quasi-periodic. In this case for many $\mu > 0$ there are infinitely many periodic orbits and also one can expect that associated to the homoclinic tangencies will be the Newhouse phenomenon of infinitely many sinks (Newhouse [36]) and behaviour similar to that of the Hénon attractor (Hénon [37]).

Now we consider all these bifurcations in a more global context. Recall that $I_{p/q}$ is the closure of the set of (ω, a) such that $P_{\omega,a}$ has an attracting periodic orbit (sink) whose rotation number is p/q. We now turn to consider the structure of $P_{\omega,a}$ when $(\omega, a) \in I_{p/q}$. The essential ideas are again captured by the simplest case where $p = 0$ and $q = 1$; i.e. a fixed point. Then our picture of what we believe happens in $I_{0/1}$ is summarised in fig. 21. The discovery of such a structure is due to Aronson, Chory, Hall and McGehee [34] who discuss this in detail for a particular two-parameter family and for the case where $p/q = 1/8$. We have only drawn one half of $I_{0/1}$ because one expects that what is happening in the other half is qualitatively similar and related by a symmetry. This is what is happening in the various regions and curves marked:

Along BA: The fixed point undergoes a saddle-node bifurcation.

In I: The invariant circle is smooth, and in the interior of I it contains a sink and a saddle. The strong stable manifold W_{sink} of the sink and the inset or stable manifold W_{sad} of the saddle intersect the boundary of the annulus in the way shown.

On α: The outset of the saddle has become cubically tangent to the local strong stable foliation of the sink.

In II: The outset of unstable manifold of the saddle is now quadratically tangent to the sink's local strong stable foliation, but does not intersect W_{sink}.

On β: The outset is quadratically tangent to W_{sink}.

In III: The outset intersects W_{sink} transversally, but does not intersect W_{sad}.

On γ: The outset intersects W_{sink} transversally and has a quadratic tangency with W_{sad}.

In IV and VII: The outset intersects W_{sink} and W_{sad} transversally.

On δ: The outset is quadratically tangent to W_{sink} as shown, and moreover, W_{sink} does not intersect one of the boundary curves of the annulus.

In V: The outset of the saddle does not intersect W_{sink}. Both branches of W_{sink} cross the same boundary curve of the annulus.

On ϕ: As in V, except that the outset of the saddle is now quadratically tangent to its inset.

In VI: As on ϕ except that the outset now intersects the inset transversally.

On τ: The outset is again quadratically tangent to the inset, but with the opposite orientation to that occuring in ϕ.

In VII: Both W_{sink} and W_{sad} cross to one side of the annulus and the saddle's outset does not intersect W_{sink} and W_{sad}. Moreover, W_{sad} separates the annulus into two invariant region.

In IX: The sink has complex conjugate eigenvalues. In crossing from I to IX the real eigenvalues of I become equal, then complex conjugate.

In X: These eigenvalues become real again.

On crossing from X into XI: There is a generic period-doubling bifurcation, and presumably a cascade of these as a is increased.

We note that the fixed point remains an attractor throughout the regions I to VIII but is not necessarily unique in III to VIII.

Now one can see why the global excitation caused by a saddle-node with a critical cycle will be ubiquitous in systems depending upon one parameter μ.

Suppose that the system starts from some phase-locked situation as in I. If it leaves I by crossing BA then the system remains quasi-periodic. Another possibility is that it leaves I by crossing α in II. If the path followed by the system then leaves II by crossing BA transversally one observes precisely the bifurcation discussed above. Thus, in this scheme, this bifurcation is the simplest mechanism for a bifurcation from quasi-periodicity to chaos.

We now discuss the relationship with maps of the circle. Each of the regions in fig. 21 except V, VI and VII has a counterpart in, for example, the following two-parameter family of maps of the

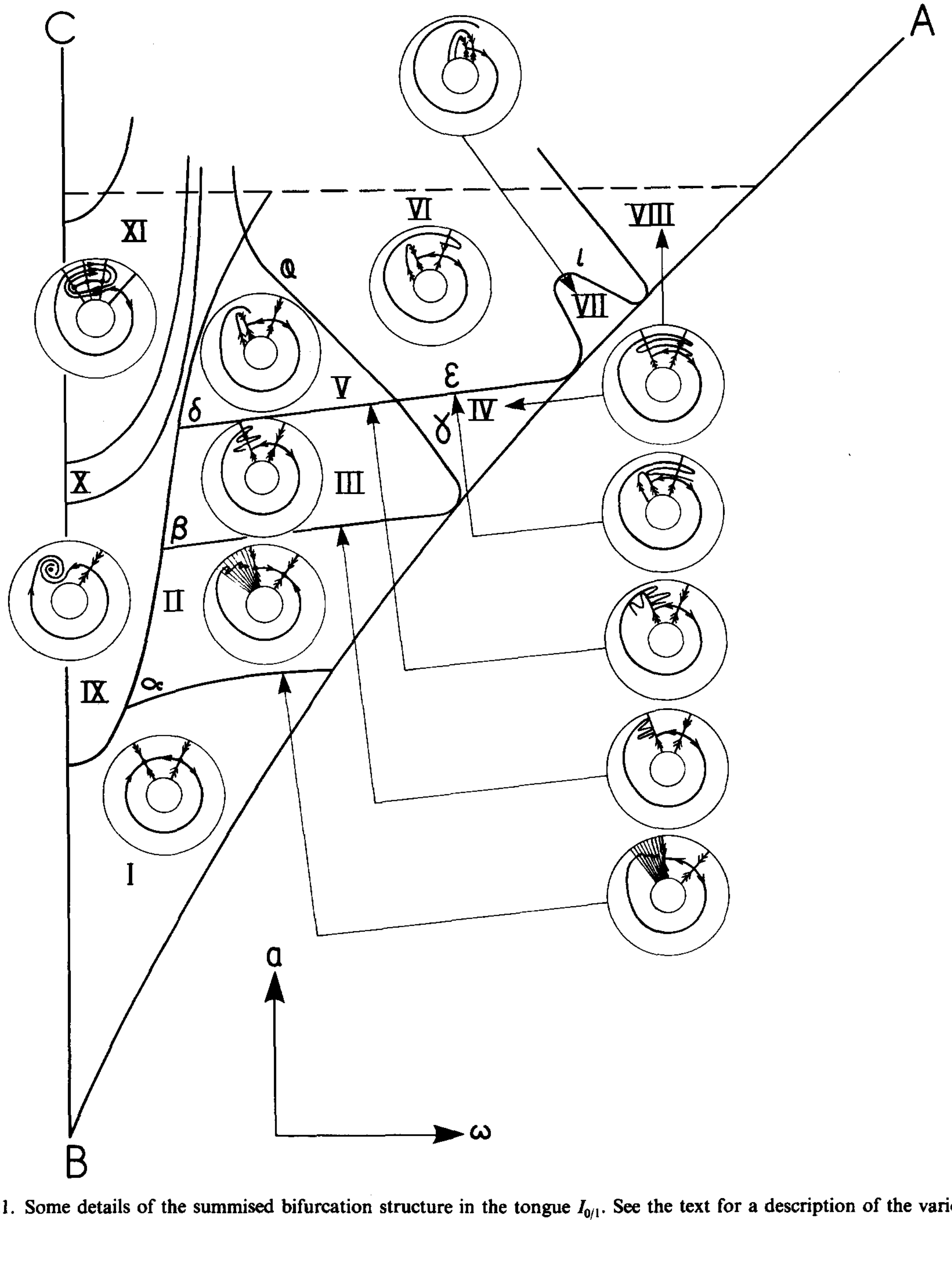

Fig. 21. Some details of the summised bifurcation structure in the tongue $I_{0/1}$. See the text for a description of the various regions.

circle:

$$f_{\omega,a}(\theta) = \theta + \omega - (a/2\pi)\sin 2\pi\theta\,,$$

though one has to be careful in the exact interpretation of this correspondence. Essentially, the correspondence is obtained by thinking of the circle mappings as the infinite-dissipation limit of the annulus mappings. All points are mapped onto a circle after one iteration; the contraction in the radial direction is infinite. On taking this limit the outset of the saddle-point converges to the circle. The strong stable foliations converge to the foliation by radial lines and points at which the outset is tangent to a stable leaf converge to images of the critical points of the circle mapping. (Of course, the sinks of the circle and annulus mappings correspond, and the saddle-point of the annulus mapping corresponds to the unstable fixed point of the circle mapping.)

We have discussed the family $f_{\omega,a}$ for $0 \leqslant a \leqslant 1$ in the previous sections. Let $I'_{0/1}$ denote the closure of the region of (ω, a)-space in which $f_{\omega,a}$ has a sink (i.e., an attracting fixed point). The region consisting of the intersection of $I'_{0/1}$ with $0 < a < 1$ corresponds to I. The curve in $I'_{0/1}$ where $a = 1$ corresponds to the upper boundary of I, so that the mappings in II and IX are respectively analogous to circle mapping like (a) and (b) in fig. 22. In fig. 22a the critical points c_1 and c_2 are such that $f^n_{\omega,a}(c_i)$, $i = 1, 2$, converge monotonically (i.e., from side to side) to the sink as $n \to \infty$. In fig. 22b they converge to the sink, but in an oscillatory manner. These properties correspond respectively to the fact that in I and II the outset of the saddle converges monotonically to the sink while in IX it spirals towards it. In III the outset has penetrated the strong stable manifold of the sink. The analogous property for the circle mappings is that the sink lies between $f_{\omega,a}(c_1)$ and $f_{\omega,a}(c_2)$ in in fig. 22c. (The stacked folds that bracket W_{sink} in region III of fig. 21 correspond to images of the two critical points.) Any annulus mapping sufficiently close to such a circle mapping will be like those in III. The circle mappings corresponding to γ have the property that $f_{\omega,a}(c_1)$ is the unstable fixed point. This corresponds to the fact that on γ the outset is tangent to the inset of the saddle. Clearly, the annulus mappings in, for example, V, have no similar 1-dimensional analogue because the strong stable manifold of the sink only meets one boundary curve of the annulus, whereas in the infinite

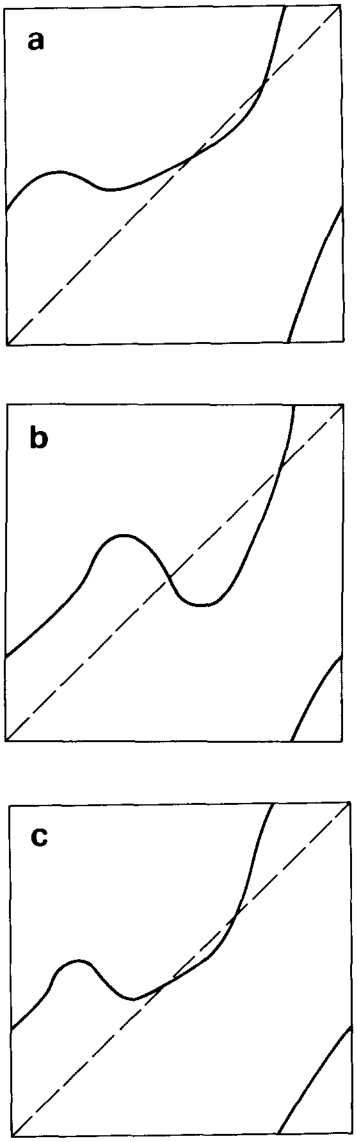

Fig. 22. Three mappings illustrating the properties described in the text.

dissipation situation this curve is a radial arc and hence meets both boundary curves of the annulus. In particular, we see that the curve γ' consisting of those (ω, a) such that $f_{\omega,a}(c_1)$ is the unstable fixed point (i.e., the analogue of γ) extends across $I'_{0/1}$ as far as the region analogous to IX. Below γ' the rotation number,

$$\rho(f, \theta) = \limsup_{n\to\infty} n^{-1}(f^n\theta - \theta)$$

of $f = f_{\omega,a}$ at θ is independent of θ and exists as a limit; while above γ it depends upon θ.

In fact, identifying numbers which differ by an integer, it can be shown that

$$R(f) = \{\rho(f, \theta): 0 \leqslant \theta \leqslant 1\}$$

is a closed interval $[\rho_-(f), \rho_+(f)]$ and that ρ_- and ρ_+ are continuous functions of f (Newhouse, Palis and Takens [35], Ito [39]). Above γ', $\rho_-(f) \neq \rho_+(f)$. In particular, there are some points θ with irrational rotation number.

Consider now the general structure of such mappings. In contrast to the diffeomorphism case (i.e., when $0 < a < 1$ for the $f_{\omega,a}$), when $a > 1$, the mapping $f = f_{\omega,a}$ always has a periodic orbit (Block and Franke [38]); thus $R(f)$ always contains a rational number. In fact, if $\rho_-(f) \neq \rho_+(f)$ then there are infinitely many unstable periodic orbits for f, because if $p/q \in R(f)$ then it is easy to show that one can solve the equation $f^q\theta = \theta + p$ and, moreover, the solution θ_0 can be chosen so that if U is any neighbourhood of θ_0 in the circle then U, $fU, \ldots, f^nU$ cover the circle for some $n \geqslant 0$ (Newhouse, Palis and Takens [35]). On the other hand $f = f_{\omega,a}$ has at most two *stable* periodic orbits, and if there are two then these contain the critical points in their basins of attraction. Moreover, from work of Jacobson [40], one expects that such mappings are structurally stable (and hence the ρ_+ and ρ_- are locally constant) if and only if the critical points are contained within the basins of

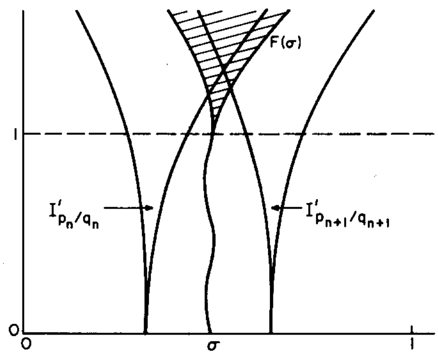

Fig. 23. The conjectured structure of $F(\sigma_G)$ and its approximation by the tongues I'_{p_n/q_n}.

stable periodic orbits. Newhouse, Palis and Takens [35] show that if f_μ is a generic one-parameter family and if μ_0 is such that not both of $\rho_+(f_\mu)$ and $\rho_-(f_\mu)$ are locally constant at μ_0 then in every neighbourhood of μ_0 there is a point μ such that for some $n > 0$ the f^n-image of a critical point is an unstable periodic point. This is the one-dimensional (infinite dissipation) analogue of a *homoclinic tangency*.

Now consider the set $F(\sigma_G)$ consisting of those points (ω, a) for which $\rho(f_{\omega,a}, \theta) = \sigma_G = (\sqrt{5} - 1)/2$ for some θ. As we have seen, for $0 < a < 1$ this is a curve of the form $\omega = u(a)$, u analytic. For $a > 1$, if $(\omega, a) \in F(\sigma_G)$ then $\rho_-(f_{\omega,a}) \neq \rho_+(f_{\omega,a})$ because $R(f_{\omega,a})$ contains a rational and an irrational. We can approximate $F(\sigma_G)$ by the regions I'_{p_n/q_n}. Therefore we expect that $F(\sigma_G)$ will have the form depicted in fig. 23. We conjecture (a) that the boundary curves of $F(\sigma_G)$ are the limit as $n \to \infty$ of boundaries of $I'_{p_{2n}/q_{2n}}$ and $I'_{p_{2n+1}/q_{2n+1}}$ and (b) that for (ω, a) in this boundary curve there is a $f_{\omega,a}$-invariant Cantor set Λ which (i) is the closure of the orbit of a critical point, (ii) is attracting, and (iii) has the property that if $\theta \in \Lambda$ then $\rho(f_{\omega,a}, \theta) = \sigma_G$. (Presumably, an invariant Cantor set satisfying (iii) exists if (ω, a) lies in the interior of $F(\sigma_G)$, but then it would not be an attractor.)

References

[1] M.J. Feigenbaum, J. Stat. Phys. 19 (1978) 25; 21 (1979) 669.

[2] G. Ahlers, in: Systems Far from Equilibrium, L. Garrido, ed. (Springer, Berlin, 1980) p. 114; G. Ahlers and R.P. Behringer, Phys. Rev. Lett. 40 (1978) 712. J.P. Gollub and S.V. Benson, J. Fluid Mech. 100 (1978) 449. R.C. DiPrima and H.L. Swinney, in: Hydrodynamic Instabilities and the Transition to Turbulence, H.L. Swinney and J.P. Gollub, eds. (Springer, Berlin, 1981) p. 139. M. Dubois and P. Bergé, J. Physique (Paris) 42 (1981) 167. A. Libchaber and J. Maurer, in: Nonlinear Phenomena at Phase Transitions and Instabilities, T. Riste, ed. (Plenum, New York, 1981).

[3] M. Hirsch, C.C. Pugh and M. Shub, Invariant Manifolds, Springer Lecture Notes # 583 (Springer, Berlin, 1977).

[4] V.I. Arnold, Translations American Mathematical Society, Second Series 46 (1965) 213.

[5] N.N. Bogoliubov and J.A. Mitropolski, Methods of Accelerated Convergence in Nonlinear Mechanics (Springer, Berlin, 1976).

[6] J. Moser, Stable and Random Motions in Dynamical Systems (Princeton Univ. Press, Princeton, 1973).

[7] M.R. Herman, Sur la Conjugaisons Differentiable des Diffeomorphismes du Cercle à des rotations, Publ. I.H.E.S. 49 (1979) 5.

[8] M.R. Herman, in: Geometry and Topology, Lecture Notes in Mathematics 597, J. Palis and M. do Carmo, eds. (Springer, Berlin, 1977) p. 271.

[9] D. Rand, S. Ostlund, J. Sethna and E.D. Siggia, Phys. Rev. Lett. 49 (1982) 132.

[10] S.J. Shenker, Physica 5D (1982) 405.

[11] M.J. Feigenbaum, L.P. Kadanoff and S.J. Shenker, Physica 5D (1982) 370.

[12] A. Denjoy, J. Math. Pures Appl. 9 (1932) 333.

[13] The set A is defined by restricting the growth rate of the entries in the continued fraction (2.3).
Specifically $\sigma \in A \Leftrightarrow$

$$\lim_{M\to\infty} \limsup_{N\to\infty} \sum_{\substack{n_i \geq M \\ 1\leq i\leq N}} \ln(1+n_i) \Big/ \sum_{1\leq i\leq N} \ln(1+n_i) = 0.$$

The set A has Lebesgue measure one on the interval, and for all $\epsilon > 0$ there exists a C_ϵ such that

$$|\sigma - p/q| \geq C_\epsilon/q^{2+\epsilon}.$$

[14] J.M. Greene, J. Math. Phys. 20 (1979) 1183.

[15] M. Nauenberg, Santa Barbara preprint, NSF-ITP-82-76 (1982).

[16] L. Jonker and D.A. Rand, Comm. Math. Phys. (to appear).

[17] P. Collet, J.P. Eckmann, O. Lanford, Comm. Math. Phys. 76 (1980) 211; P. Collet and J.P. Eckmann, Iterated Maps on the Interval as Dynamical Systems (Birkhäuser, Boston, 1980).

[18] O. Lanford, Bull. Amer. Math. Soc. 6 (1982) 427.

[19] M. Campanino, H. Epstein and D. Ruelle, Comm. Math. Phys. 79 (1981) 261; and Topology 21 (1983) 125.

[20] To avoid cumbersome notation we have not used the composition symbol where our intention is clear. Thus we write $\xi \circ \eta$ as $\xi\eta$, etc.

[21] R. McKay, private communication.

[22] For this argument we need T to be defined on a full neighbourhood of (ξ_*, η_*). This is achieved by dropping the condition that ξ and η are monotonic.

[23] P. Billingsley, Ergodic Theory and Information (Wiley, New York, 1965).

[24] W. Osceledeč, Trudy Mosk. Mat. Obsc. 19 (1968) 679. D. Ruelle, Ergodic Theory of Differentiable Dynamical Systems, Publ. Math. I.H.E.S. 50 (1979) 27.

[25] P. Collet, J.P. Eckmann and H. Koch, J. Stat. Phys. 25 (1981) 1.

[26] M. Gorman, H.L. Swinney and D. Rand, Phys. Rev. Lett. 46 (1981) 992. D. Rand Arch. Rat. Mech. Anal. 79 (1982) 1.

[27] D. Ruelle and F. Takens, Comm. Math. Phys. 20 (1971) 167.

[28] D.F. Escande and F. Doveil, J. Stat. Phys. 26 (1981) 257.

[29] L.P. Kadanoff, Phys. Rev. Lett. 47 (1981) 1641; S.J. Shenker and L.P. Kadanoff, J. Stat. Phys. 27 (1982) 631.

[30] B. Simon, Adv. Appl. Math. (to appear).

[31] D.R. Hofstadter, Phys. Rev. B 14 (1976) 2239.

[32] M.J. Feigenbaum and B. Hasslacher, Phys. Rev. Lett. 49 (1982) 605.

[33] N. Manton and M. Nauenberg, Santa Barbara preprint Comm. Math. Phys. (to appear).

[34] D.G. Aronson, M.A. Chory, G.R. Hall and R.P. McGehee, Comm. Math. Phys. 83 (1982) 303 (see in particular p. 341, fig. 9.1).

[35] S. Newhouse, J. Palis and F. Takens, preprint (1980) (see particularly section 3C).

[36] S. Newhouse, The Abundance of Wild Hyperbolid Sets and Non-smooth Stable Sets, Publ. Math. I.H.E.S. (Paris) 50 (1979) 101.

[37] M. Hénon, Comm. Math. Phys. 50 (1976) 69.

[38] L. Block and J. Franke, Invent. Math. 22 (1973) 69.

[39] R. Ito, Math. Proc. Camb. Phil. Soc. 89 (1980) 107.

[40] M. Jacobson, Math. U.S.S.R. Sbornik 14 (1971) 161.